AD NUMBER
AD093432
CLASSIFICATION CHANGES
TO: **unclassified**
FROM: **secret**
LIMITATION CHANGES
TO: **Approved for public release, distribution unlimited**
FROM: **Controlling Organization: The British Embassy, 3100 Massachusetts Avenue, NW, Washington, DC 20008.**
AUTHORITY
DSTL, AVIA 6/19793, 22 Oct 2009; DSTL, AVIA 6/19793, 22 Oct 2009

NOTICE: THIS DOCUMENT CONTAINS INFORMATION AFFECTING THE NATIONAL DEFENSE OF THE UNITED STATES WITHIN THE MEANING OF THE ESPIONAGE LAWS, TITLE 18, U.S.C., SECTIONS 793 and 794. THE TRANSMISSION OR THE REVELATION OF ITS CONTENTS IN ANY MANNER TO AN UNAUTHORIZED PERSON IS PROHIBITED BY LAW.

SECRET

ROYAL AIRCRAFT ESTABLISHMENT

FARNBOROUGH, HANTS.

TECHNICAL NOTE No: G.W.397

PRELIMINARY DESIGN AND ANALYSIS OF HEADING CONTROL SYSTEMS FOR A JET CONTROLLED TEST VEHICLE (RTV1 J)

by

A.P.MacLAREN, B.Sc., A.M.I.E.E. and
J.H.W.SHANNON, B.E.(Mech.), B.E.(Aero.)

JANUARY, 1956

MINISTRY OF SUPPLY

SECRET

U.D.C. No. 623.451-519 : 629.13.014.59 : 533.691.155.8 : 533.665

Technical Note No. GW 397

January, 1956

ROYAL AIRCRAFT ESTABLISHMENT, FARNBOROUGH

Preliminary Design and Analysis of Heading Control Systems for a Jet Controlled Test Vehicle (RTV1 J)

by

A. P. MacLaren, B.Sc., A.M.I.E.E.

and

J. H. W. Shannon, B.E.(Mech.), B.E.(Aero.).

SUMMARY

As part of the supporting experimental programme for ballistic missile development, it is intended to control the heading of unboosted, vertically-launched, wingless RTV1 missiles by means of rocket motor deflection. A separate system of air jets will be used for roll stabilisation.

This note describes in some detail the preliminary design and analysis of the proposed pitch and yaw control system. Frequency response techniques are used in the basic design of the system. From this analysis, in which aerodynamic forces are neglected, suitable values of loop gain for a range of rocket motor servo bandwidths are determined. Two possible systems, with and without integral of error control, are considered and their relative merits are illustrated by comparing the deviations from a vertical trajectory caused by an initial heading error and a control system bias. These simplified trajectory calculations indicate that the control system including integral of error is to be preferred. In the final section, the effects of aerodynamic forces, under particular conditions of flight, on the stability of the proposed system are examined.

It is concluded that a stable heading control system for aerodynamically unstable RTV1 test vehicles can be developed along the lines proposed in this note, without demanding excessively high component performances. Further work will include studies of the effects of body flexure on the stability of the system and simulator tests in which some of the actual components will be incorporated in the control loop.

LIST OF CONTENTS

LIST OF APPENDICES

LIST OF ILLUSTRATIONS

LIST OF ILLUSTRATIONS (Contd)

1 Introduction

In flight trials to study the use of rocket motor deflection as a means of control[1], it is proposed that modified RTV1 test vehicles shall be launched vertically from a zero length launcher. No boost will be used and the missile longitudinal acceleration at take-off will be less than 1g. For a typical case a thrust duration of 24 seconds may be expected to give a speed of the order of 700 ft/sec and an altitude of about 8,000 ft at all-burnt. In these experiments, there will be an initial period of flight in which the aerodynamic forces will be negligible. In this note, therefore, the analysis on which the control system design is based has been simplified by neglecting aerodynamic forces in the first instance. The effect of aerodynamic forces on the performance of the proposed control system, for one particular flight condition, is examined subsequently. For these trials the normal RTV1 wings and fins will be removed and consequently the modified vehicle will be aerodynamically unstable.

The missile will be roll stabilised to a gyro datum by means of a separate system of air jets. The design of the latter is outside the scope of this note. For lateral control the missile heading angle will be controlled in two orthogonal planes, referred to as the pitch and yaw planes. As the configuration is symmetrical, control in one plane only is considered, the system in the other plane being assumed to be identical. Cross-coupling effects are not included in the analysis as no reliable data on these are available.

Two possible types of lateral control system are considered. In the first, rocket motor deflection proportional to heading angle error, sensed by a free gyroscope, is used with rate feedback from a rate gyroscope for damping. This is the simplest system which will give stable flight. The second is similar to the first with the addition of a signal proportional to the integral of heading angle error to eliminate steady state errors. Block diagrams of the two types of system are shown in Figs. 1 and 2. Frequency response techniques, which are generally employed in the analysis of linear servomechanisms, are used in the basic design of the system. The transfer functions of the rate gyroscope and the motor position control servo are assumed, for this purpose, to be simple quadratic functions. In the design of the system, three possible motor servo bandwidths, corresponding to natural frequencies of 3, 5 and 10 cycles per second, are examined to show the effect of this parameter on the permissible values of loop gain for a well damped transient response. These bandwidths are thought reasonable in the light of existing hydraulic servo development. Some relevant design work is described in Ref.2.

In section 3 the lateral motions arising from an error in missile attitude at the instant of launch and from a constant rocket motor deflection bias are calculated for the two types of system. These calculations based on certain simplifying assumptions, indicate that the system including integral of error is more effective in reducing deviations from the desired course and is therefore to be preferred. The stability of this system with missile aerodynamics included is analysed in section 4.

2 Control System Analysis Neglecting Aerodynamic Forces

2.1 Response of the missile to rocket motor deflection

Referring to Fig.3, it can be seen that the equation of missile angular motion in the yaw plane when aerodynamic forces are negligible, may be written

$$C\ddot{\psi} = -T\ell\delta \qquad (1)$$

where the dot notation indicates differentiation with respect to time

and ψ = the missile heading angle with respect to a fixed direction (assumed vertical),

δ = the rocket motor deflection measured from the missile axis (assumed small so that $\sin \delta \doteq \delta$),

T = the rocket motor thrust,

C = the missile lateral moment of inertia about an axis through the centre of gravity,

ℓ = the distance between the missile centre of gravity and the rocket motor pivot point.

Re-writing equation (1) in the form of a transfer function we have

$$\frac{\bar{\dot{\psi}}}{\bar{\delta}} = -\frac{K_4}{p} = -K_4 G_4 \qquad (2)$$

where $K_4 = \frac{T\ell}{C}$ = the invariant factor of the transfer function,

and $G_4 = \frac{1}{p}$ = the frequency variant part of the transfer function.

$\bar{\dot{\psi}}$ and $\bar{\delta}$ denote the Laplace transforms of $\dot{\psi}$ and δ respectively.

2.2 Transfer functions of the servo and rate gyroscope

It is assumed that the closed-loop transfer function of the rocket motor position control servomechanism can be represented by a quadratic function of the form

$$\frac{\bar{\delta}}{\bar{e}_3} = -K_3 G_3 = -\frac{K_3 \omega_3^2}{p^2 + 2\zeta_3 \omega_3 p + \omega_3^2} \qquad (3)$$

where e_3 = the input signal to the servo,

K_3 = the invariant factor of the transfer function,

G_3 = the frequency variant part of the transfer function,

ω_3 = 2π x the undamped natural frequency f_3,

ζ_3 = the damping factor.

To show the effect of different servo bandwidths on the permissible values of heading control stiffness, three values of the undamped natural frequency f_3, namely 3, 5 and 10 cycles per second have been used in the analysis. The damping factor ζ_3 is assumed equal to 0.6 throughout.

For the rate gyroscope a quadratic transfer is also assumed, namely

$$\frac{\bar{e}_2}{\bar{\dot{\psi}}} = K_2 G_2 = \frac{K_2 \omega_2^2}{p^2 + 2\zeta_2 \omega_2 p + \omega_2^2} \qquad (4)$$

where e_2 = the output signal from the rate gyroscope,

K_2 and G_2 = the invariant and frequency variant parts of the transfer function respectively,

ω_2 = 2π x the undamped natural frequency f_2,

ζ_2 = the damping factor.

The values used for f_2 and ζ_2 are respectively 29 cycles per second and 0.5. These are related to an existing rate gyroscope which has a range of $\pm 60^\circ$ per second.

Fig.4 shows the frequency response curves corresponding to the transfer functions assumed for the servo and rate gyro. The values of the gain parameters K_2 and K_3 are assumed to be at our disposal.

2.3 Frequency response study of control system without integral of error

It can be seen from the block diagram of Fig.1 that the inner loop feedback transfer function is given by

$$\frac{\bar{e}_2}{\bar{e}_3} = \frac{\bar{e}_2}{\bar{\psi}} \cdot \frac{\bar{\psi}}{\bar{\delta}} \cdot \frac{\bar{\delta}}{\bar{e}_3} = K_2G_2 \cdot K_3G_3 \cdot K_4G_4 \cdot \qquad (5)$$

The frequency variant part $(G_2G_3G_4)$ of the transfer function of expression (5) is plotted in Fig.5. Three sets of curves are shown corresponding to the three assumed servo frequencies of 3, 5 and 10 cycles per second. It can be seen by plotting gain/phase curves on a Nichol's chart that the closed loop response of the rate feedback loop will be adequately damped if a phase margin of 60° is maintained in each case. For this condition the following loop gains and stability margins are obtained.

Table I

Rate Feedback Loop Gains

Servo bandwidth f_3 cycles per second	3	5	10
Loop gain in db $(20 \log_{10} L_1)$	17.0	21.0	26.0
Loop gain factor $L_1 = K_2K_3K_4$	7.08	11.2	20.0
Loop gain margin	9.1 db at 2.82 c/s	8.6 db at 4.52 c/s	8.3 db at 8.25 c/s
Loop phase margin	60° at 1.14 c/s	60° at 1.81 c/s	60° at 3.26 c/s

With the rate feedback loop closed we have

$$e_3 = e_1 - e_2 \qquad (6)$$

and the closed loop transfer function may be expressed as

$$\frac{\dot{\psi}}{\dot{e}_1} = \frac{1}{K_2G_2}\left[\frac{K_2G_2K_3G_3K_4G_4}{1 + K_2G_2K_3G_3K_4G_4}\right] \qquad (7)$$

where e_1 = the output signal from the heading angle gyroscope. The feedback transfer function for the position feedback loop is given by

$$\frac{\dot{\psi}}{\dot{\psi}_\varepsilon} = \frac{K_1}{pK_2G_2}\left[\frac{K_2G_2K_3G_3K_4G_4}{1 + K_2G_2K_3G_3K_4G_4}\right] \qquad (8)$$

where ψ_ε denotes the heading angle error from the gyro datum and K_1 is the gain factor for heading angle error signal.

Gain and phase plots representing the frequency variant part of the above transfer function, incorporating the appropriate rate loop gains given in Table I for the three cases, are shown in Fig.6. Inspection of these on a Nichol's chart shows that a well damped closed loop response will be obtained with a phase margin of 60°. The following loop gains and stability margins are obtained for this condition.

Table II

Position Feedback Loop Gains

Servo bandwidth f_3 cycles per second	3	5	10
Loop gain in db ($20 \log_{10} L_2$)	11.0	14.8	19.6
Loop gain factor $L_2 = \frac{K_1}{K_2}$	3.55	5.50	9.55
Loop gain margin	8.7 db at 1.60 c/s	9.1 db at 2.48 c/s	8.9 db at 4.30 c/s
Loop phase margin	60° at 0.58 c/s	60° at 0.88 c/s	60° at 1.50 c/s

Fig.7 shows the variation with frequency of the gain of the closed loop transfer function $\frac{\dot{\psi}}{\dot{\psi}_D}$ for the three cases. ψ_D denotes the gyro datum angle measured with respect to the same fixed direction as ψ.

2.4 Frequency response study of control system with integral of error

As the rate feedback loop transfer function is identical with that already studied in section 2.3, the loop gains set out in Table I also apply to the control system illustrated by Fig.2. In this case, however, the position feedback loop includes an additional term proportional to integral of heading angle error and hence the feedback transfer function of this loop becomes

$$\frac{\bar{\psi}}{\bar{\psi}_\varepsilon} = \frac{K_5}{K_2} \cdot \frac{\left(1 + p\frac{K_1}{K_5}\right)}{p^2 G_2} \left[\frac{K_2G_2K_3G_3K_4G_4}{1 + K_2G_2K_3G_3K_4G_4}\right] \qquad (9)$$

where K_5 denotes the gain factor of the integrator.

The frequency response of the term $\frac{1}{p^2G_2}\left[\frac{K_2G_2K_3G_3K_4G_4}{1 + K_2G_2K_3G_3K_4G_4}\right]$ is shown in Fig.8. The parameters of the remaining part of the transfer function of expression (9) $\frac{K_5}{K_2}\left(1 + p\frac{K_1}{K_5}\right)$ are at our disposal to be chosen in such a way that the response of the outer loop is satisfactory. Since there are two parameters at our disposal, namely K_1 and K_5, the transfer function of expression (9) may be made to satisfy two conditions. To facilitate comparison between the types of system shown in Figs. 1 and 2, the criterion of 60° phase margin in the outer loop, used in section 2.3, is retained as the first of these conditions. The second condition selected is that K_5, the integrator gain factor, shall be as large as possible, compatible with the first condition being fulfilled, to reduce errors due to low frequency disturbances to a minimum.

The method used to determine the values of K_5 and K_1 to satisfy these conditions is as follows. Consider first the frequency response of the term $\left(1 + p\frac{K_1}{K_5}\right)$ illustrated in Fig.9. This has a break frequency, as yet undetermined at $\omega_o = \frac{K_5}{K_1}$. Above this frequency the gain asymptote rises at 6 db per octave and the phase lead increases from 45° to 90°. Let D_1 and ϕ_1 denote respectively the gain (in db) and phase of the term $\left(1 + p\frac{K_1}{K_5}\right)$ at the outer loop cut-off frequency ω_o i.e. the frequency at which the feedback gain is unity (zero db). Then to fulfil the 60° phase margin condition the following equations must be satisfied:-

$$20 \log_{10} \frac{K_5}{K_2} + D_1 + D_2 = 0 \quad \text{(db)} \qquad (10)$$

$$\phi_1 + \phi_2 = -120 \quad \text{(degrees)} \qquad (11)$$

where D_2 and ϕ_2 denote respectively the gain in db and the phase of the term $\frac{1}{p^2G_2}\left[\frac{K_2G_2K_3G_3K_4G_4}{1 + K_2G_2K_3G_3K_4G_4}\right]$ at the out-off frequency ω_o.

The out-off frequency ω_o corresponding to any particular value of ϕ_1 is easily determined by means of equation (11) and the phase curve of Fig.8. The gain D_2 corresponding to any value of ω_o can be read from the gain curve of Fig.8. For example, for $\phi_1 = 80^\circ$, $\phi_2 = -200^\circ$ from equation (11) and from Fig.8 it can be seen that $\omega_o = 3.72$ radians per second and $D_2 = -22.7$ db for a servo natural frequency of 5 cycles per second. The nine

values of ω_c and the corresponding values of D_2 for the three servo bandwidths and for $\phi_1 = 75^\circ$, 80° and 85° are given in Table III. From Fig.9 it can be seen that the values of D_1 corresponding to $\phi_1 = 75^\circ$, 80° and 85° are 11.8 db at a frequency of $3.75\ \omega_o$, 15.3 db at $5.8\ \omega_o$ and 21.2 db at $11.6\ \omega_o$. Since these are the cut-off frequencies we have:-

$$\frac{K_5}{K_1} = \omega_o = \frac{\omega_c}{3.75}, \frac{\omega_c}{5.8} \text{ or } \frac{\omega_c}{11.6} \text{ for } \phi_1 = 75^\circ, 80^\circ \text{ or } 85^\circ \text{ respectively.} \quad (12)$$

The nine values of the ratio $\frac{K_5}{K_1}$ given in Table III are derived from equation (12) by using the appropriate value of ω_c and the corresponding values of $\frac{K_5}{K_2}$ are obtained from equation (10). Hence the values of K_1 and K_5 corresponding to the three values of ϕ_1 are determined since K_2 is fixed by the rate feedback loop gain given in Table I.

Table III

Values of K_1 and K_5 corresponding to the three values of ϕ_1

Phase ϕ_1 degrees	+75			+80			+85		
Gain D_1 db	+11.8			+15.3			+21.2		
Ratio $\frac{\omega_c}{\omega_o}$	3.75			5.80			11.6		
Phase ϕ_2 degrees	-195			-200			-205		
Servo bandwidth f_3 c/s	3	5	10	3	5	10	3	5	10
Cut-off frequency ω_c rad/sec	1.80	2.85	4.85	2.33	3.72	6.35	2.90	4.65	8.00
$\omega_o \left(= \frac{K_5}{K_1}\right)$ rad/sec	0.480	0.760	1.29	0.402	0.642	1.10	0.250	0.402	0.690
Gain D_2 db	-10.2	-18.2	-27.3	-14.7	-22.7	-32.2	-18.5	-26.5	-36.2
$20 \log_{10} \frac{K_5}{K_2}$	-1.6	+6.4	+15.5	-0.6	+7.4	+16.9	-2.7	+5.3	+15.0
Ratio $\frac{K_5}{K_2}$	0.832	2.09	5.96	0.933	2.34	7.00	0.733	1.84	5.62
Ratio $\frac{K_1}{K_2}$	1.73	2.75	4.62	2.32	3.64	6.37	2.94	4.58	8.14

All the values of $\frac{K_5}{K_2}$ and $\frac{K_1}{K_2}$ given in Table III satisfy the first (60° phase margin) condition. Comparison of the values of $\frac{K_1}{K_2}$, given in Table II, for the system without integral of error with the corresponding values in Table III shows that the latter are lower. For predetermined values

of K_2, K_1 increases with ϕ_1 tending to the values given in Table II as ϕ_1 tends to 90° and K_5 tends to zero. It can be seen from Table III, however, that for all three servo bandwidths K_5 is larger for $\phi_1 = 80°$ than for $\phi_1 = 75°$ or 85°. Thus K_5 has a maximum value in the region of $\phi_1 = 80°$. The values of K_1 and K_5 given in the three central columns therefore satisfy approximately both the chosen conditions and will be used in all subsequent calculations on the integral of error system.

The process of determining the values of K_5 and K_1 which satisfy the conditions selected can be carried out quickly and conveniently by using templates cut to the shape of the gain and phase curves of Fig.9.

The frequency response curves for the outer loop feedback transfer function for the three servos and for $\phi_1 = 80°$ are shown in Fig.10. It can be seen from this that the gain margin is 12.4 db at 1.56, 2.42 and 4.15 cycles per second, the phase margin being 60° at 0.37, 0.59 and 1.01 cycles per second, for $f_3 = 3$, 5 and 10 cycles per second respectively. Fig.11 shows a comparison of the frequency responses for $\phi_1 = 80°$ and $\phi_1 = 85°$ for $f_3 = 10$ cycles per second. It is evident that $\phi_1 = 80°$ gives a higher gain at low frequencies, due to the higher integrator gain factor, at the expense of a rather lower gain at high frequencies. The variation with frequency of the gain of the closed loop transfer function $\frac{\Psi}{\Psi_D}$ for the three servo bandwidths is shown in Fig.12. Polar plots for $f_3 = 10$ cycles per second for the two types of system shown in Figs. 1 and 2 are compared in Fig.13.

2.5 Numerical values of gain factors for the proposed control systems

The values given in this section are based on the frequency response studies of sections 2.3 and 2.4 and on the following data for the RTV1 missile.

Table IV

Assumed Missile Parameters

Fuel Condition	Mass m slugs	Moment of Inertia C slug ft²	Centre of gravity position aft of nose ft	Rocket motor pivot aft of centre of gravity ℓ ft	Assumed Motor Thrust T lb	$K_4 = \frac{T\ell}{C}$	
						radians per sec² per rad	radians per sec² per deg
Tanks full	17.6	352	8.94	7.79	1000	22.1	0.386
Half full	15.6	346	8.85	7.88	1000	22.8	0.397
Tanks empty	13.5	328	8.55	8.19	1000	25.0	0.436

In calculating the values of K_1, K_2 and K_5 given in the following tables, K_3 is assumed equal to unity (one degree of motor deflection per volt). The actual value assumed is unimportant since, for given values of K_4 and the feedback loop gains, the products $K_1 K_3$, $K_2 K_3$ and $K_5 K_3$ will be constant. By choosing K_3 as unity, the value, for instance, of K_1 in volts per degree is numerically the same as that of the product $K_1 K_3$ in degrees of motor deflection per degree of heading angle error.

The parameters for the control system of Fig.1 are based on the loop gains given in Tables I and II.

Table V

Parameters for the Control System of Fig.1

Fuel Condition	K_3 deg/volt	K_4 sec^{-2}	f_3 = 3 cycles per sec		f_3 = 5 cycles per sec		f_3 = 10 cycles per sec	
			K_2 V/deg/sec	K_1 V/deg	K_2 V/deg/sec	K_1 V/deg	K_2 V/deg/sec	K_1 V/deg
Full	1.0	22.1	0.318	1.13	0.507	2.79	0.905	8.64
Hall full	1.0	22.8	0.311	1.10	0.493	2.72	0.880	8.40
Empty	1.0	25.0	0.284	1.01	0.449	2.47	0.800	7.64

The parameters for the control system of Fig.2 are based on the gain ratios $\frac{K_5}{K_2}$ and $\frac{K_1}{K_2}$ given in the central columns of Table III. The values of K_2, K_3 and K_4 are the same as those given in Table V above.

Table VI

Parameters for the Control System of Fig.2

Fuel Condition	f_3 = 3 cycles per sec		f_3 = 5 cycles per sec		f_3 = 10 cycles per sec	
	K_5 V/sec/deg	K_1 V/deg	K_5 V/sec/deg	K_1 V/deg	K_5 V/sec/deg	K_1 V/deg
Full	0.297	0.738	1.19	1.84	6.33	5.76
Half full	0.290	0.722	1.15	1.79	6.16	5.60
Empty	0.265	0.658	1.05	1.64	5.60	5.10

It can be seen from the above tables that, if the feedback gain factors are kept constant throughout flight, the loop gains will increase as the flight proceeds by approximately 13%, i.e. about 1 db, due to reduction in the moment of inertia etc. This is unlikely to have serious effects in view of the large gain and phase margins available. In the following sections of this note, therefore, it is assumed that the feedback gain factors K_1, K_2, K_3 and K_5 will be kept constant at the values given in Tables V and VI for tanks full conditions.

3 Effect of Control System Parameters on Test Vehicle Behaviour

The optimum control system may be defined as that which allows the missile to deviate, under the influence of external disturbing forces and imperfections in the missile, by the least amount from the desired trajectory. Calculation of trajectories resulting from a variety of input demands, initial conditions, disturbing forces, winds, etc, is a formidable task which may be more conveniently performed by means of electronic computors. In this work, therefore, no attempt has been made to determine the optimum control system as defined above, but, in order to illustrate the effect of the control system parameters on the trajectory, the missile motion resulting from two types of imperfection has been calculated.

These illustrative calculations are based on the system parameters given in Tables IV, V and VI of section 2.5 and on the following simplifying assumptions:-

(i) that the demanded heading angle ψ_D remains vertical throughout flight;

(ii) that the angles ψ_ε and δ are small. The rocket motor deflection δ is assumed to be limited to $\pm 5^\circ$;

(iii) that the missile mass, centre of gravity, moment of inertia and feedback gain factors remain constant at the value corresponding to tanks full conditions;

(iv) that aerodynamic forces can be neglected;

(v) that the rate gyroscope and rocket motor servo lags can be neglected.

The deviation of the missile from the ideal vertical trajectory has been calculated for the following two cases:-

(a) the missile has an initial heading angle error of 3° with respect to the vertical datum;

(b) a constant rocket motor deflection bias of 1° is present in the control system.

The details of these calculations are set out in Appendix I and the results are summarised in sections 3.2 and 3.3.

3.1 Basic equations

The assumptions stated above enable the missile motion to be expressed in terms of low-order linear differential equations with constant coefficients, the solution of which is readily obtainable by the Laplace Transformation method. From equation (1), the angular motion neglecting aerodynamic forces, is given by

$$\ddot{\psi} = -\frac{T\ell}{C}\delta = -K_4\delta \qquad (13)$$

where K_4 is constant and equal to 22.13 by assumption (iii).

By assumption (v), the control equation for the system without integral of error (Fig.1) can be written

$$\delta = -K_3(e_1 - e_2) = -K_1K_3\psi_\varepsilon + K_2K_3\dot{\psi} \ . \qquad (14)$$

Now

$$\psi_\varepsilon = (\psi_D - \psi) = -\psi \qquad (15)$$

since by assumption (i) $\psi_D = 0$, both ψ and ψ_D being measured with respect to a vertical datum. Hence (14) becomes

$$\delta = K_1K_3\psi + K_2K_3\dot{\psi} \ . \qquad (16)$$

Similarly the control equation for the system with integral of error reduces to

$$\delta = K_5K_3 \int \psi \, dt + K_1K_3\psi + K_2K_3\dot{\psi} . \qquad (17)$$

The horizontal component of missile acceleration is given by

$$\ddot{x} = \frac{T}{m} \sin(\psi + \delta) \doteq \frac{T}{m}(\psi + \delta) \qquad (18)$$

by assumption (ii), and the vertical component by

$$\ddot{y} = \frac{T}{m} \cos(\psi + \delta) - g \doteq \left(\frac{T}{m} - g\right) . \qquad (19)$$

The coordinates (x,y) denote the position in space of the missile centre of gravity with respect to its position at the instant of launch; g is the acceleration due to gravity and m the mass of the rocket.

3.2 Missile deviation due to a 3° initial heading angle error

(a) Control system of Fig.1 (without integral of error)

The results of the trajectory calculations for this case, shown graphically in Fig.14, are given in Tables VIII and IX of the Appendix. It can be seen from the latter that, although the initial heading error decreases exponentially to zero, the transient angular motion results in a steady state crossing velocity $\dot{x}$. The heading angle error is reduced to 2% of its initial value in 1.20, 0.777 and 0.526 sec for the loop gains chosen for f_3 = 3, 5 and 10 c/s respectively and the corresponding steady state crossing velocities are 0.834, 0.573 and 0.486 ft/sec. If the motor deflection limit is not reached, the crossing velocity is proportional to the initial heading angle error.

(b) Control system of Fig.2 (with integral of error)

The results for this case are illustrated in Fig.15 and given in numerical form in Tables X and XI of the Appendix. Again the heading error decreases exponentially to zero but the response of this system is slower. For instance, the heading angle error is reduced to 2% of its initial value in 5.55, 3.48 and 1.75 sec for f_3 = 3, 5 and 10 c/s respectively. On the other hand, unless the motor deflection limit is reached during the initial transient, no steady state crossing velocity $\dot{x}$ occurs with this system. A small position error arises instead. The crossing rates of 0.047 and 0.46 ft/sec, which occur with the gain parameters corresponding to f_3 = 5 and 10 c/s respectively, are due to the effects of limiting the motor deflection.

3.3 Missile deviation due to a 1° motor deflection bias

(a) Control system of Fig.1 (without integral of error)

The trajectories calculated for this case are illustrated in Fig.16 and given in functional form in Table XII in the Appendix. It can be seen that with this system a 1° bias causes steady state heading errors of 0.88°, 0.36° and 0.116° for the gain parameters corresponding to f_3 = 3, 5 and 10 c/s respectively. There is, in consequence, a steady transverse acceleration $\ddot{x}$ of 0.87, 0.353 and 0.115 ft/sec^2. The magnitude of this acceleration is directly proportional to the bias angle.

(b) Control system of Fig.2 (with integral of error)

The trajectories for this case are shown in Fig.17 and given in Table XIII in the Appendix. It can be seen from the form of expression (I.31) that no

steady state heading angle error results from a constant bias in this type of control system. Consequently there is no steady state transverse acceleration $\ddot{x}$ but, as can be seen from Table XIII the transient angular motion results in a steady crossing velocity $\dot{x}$ of 3.30, 0.83 and 0.157 ft/sec for the gain parameters corresponding to f_3 = 3, 5 and 10 c/s respectively. This crossing rate is directly proportional to the bias, provided that limiting does not occur.

3.4 Discussion of results

It has been shown that without an integral of heading angle error term in the control equation a steady state component of velocity normal to the desired trajectory arises from an error in launching attitude, whereas with integral of error control a position error arises but no steady crossing velocity, provided that motor deflection limiting does not occur. Similarly a bias in the control system causes a steady state transverse acceleration without integral control whereas with integral control a transverse velocity arises but no steady lateral acceleration. Thus it appears that the system with integral of error control, in spite of its slower transient response characteristics, tends to give smaller deviations from the desired trajectory due to disturbances. The advantage of the integral control system becomes more marked as the time of controlled flight increases since the ratio of the lateral displacements arising from a given disturbance increases with time.

The effect of the higher loop gains, which are permissible with increased servo bandwidth, can be seen from Figs. 14, 15, 16 and 17. In all cases, where limiting does not seriously affect the result, the displacement from the desired trajectory due to a given disturbance becomes less as the bandwidth and gain increase. Fig.15 shows an example (f_3 = 10 c/s) of how this general tendency can be offset by the adverse effects of motor deflection limiting. It appears desirable, therefore, to avoid using such high values of loop gain that the probable range of disturbances will cause excessive limiting.

4 Control System Analysis Including Aerodynamic Forces

The following analysis is intended to illustrate the effects of aerodynamic forces and moments on the stability of the integral of error control system. Since the vehicle is symmetrical and roll stabilised, the analysis may be simplified, as in section 2, by considering motion in one plane only. Aerodynamic and jet control forces are expressed with reference to missile axes, gravitational forces and effects arising from varying flight path velocity being neglected. Theoretical estimates, by Chapman, of the normal force coefficient and centre of pressure position for the wingless RTV1 configuration at subsonic speeds show non-linear variations with incidence of the normal force and yawing moment. For the purpose of the following dynamic stability analysis, we have considered the effects of small perturbations about fixed values of incidence and have assumed linear relations over this limited range. The missile is aerodynamically unstable for small angles of incidence.

4.1 Response of the missile to rocket motor deflection

The basic equations of motion in the yaw plane are

$$\left.\begin{aligned} m(\dot{v} + Ur) &= Y \\ C\dot{r} &= N \end{aligned}\right\} \qquad (20)$$

where v and r denote the sideslip velocity and rate of turn respectively, m the mass and U the flight path velocity. Y and N denote respectively the normal force and moment acting in the yaw plane. Taking total differentials of equations (20) gives

$$\left.\begin{aligned} m\,(\dot{dv} + U\dot{dr}) &= \frac{\partial Y}{\partial v}\,dv + \frac{\partial Y}{\partial r}\,dr + \frac{\partial Y}{\partial \delta}\,d\delta \\ C\dot{dr} &= \frac{\partial N}{\partial v}\,dv + \frac{\partial N}{\partial r}\,dr + \frac{\partial N}{\partial \delta}\,d\delta\,. \end{aligned}\right\} \qquad (21)$$

Writing $\frac{\partial Y}{\partial v} = Y_v$, $\frac{\partial Y}{\partial \delta} = Y_\delta$ etc, neglecting Y_r and N_r and denoting perturbations by dashes, i.e. $dr = r'$, $dv = v'$ etc, equations (21) become

$$\left.\begin{aligned} m\,(\dot{v}' + Ur') &= Y_v v' + Y_\delta \delta' \\ C\dot{r}' &= N_v v' + N_\delta \delta'. \end{aligned}\right\} \qquad (22)$$

Transforming equations (22) and eliminating $\bar{v}'$ gives the transfer function

$$\frac{\bar{r}'}{\bar{\delta}'} = \frac{\bar{\dot{\psi}}'}{\bar{\delta}'} = \frac{n_\delta p + n_v y_\delta - y_v n_\delta}{p^2 - y_v p + U n_v} \qquad (23)$$

where $y_v = \frac{Y_v}{m}$, $n_v = \frac{N_v}{C}$, $y = \frac{Y_\delta}{m}$, $n = \frac{N_\delta}{C}$ and $r = \dot{\psi}$.

The estimated values of the coefficients of expression (23) are given in Table VII for $U = 300$ ft/sec and incidences of 0° and 10°. Missile conditions assumed, corresponding to tanks half full, are $m = 15.6$ slugs, $C = 346$ slug ft^2 and centre of gravity 8.85 ft aft of the nose (Table IV), since the speed half way through powered flight will be in the region of 300 ft/sec.

Table VII

Aerodynamic Derivatives for Wingless RTV1 at 300 ft/sec

Incidence β	y_r	n_v	y_δ	n_δ
0°	-0.0185	-0.0138	64.2	-22.8
10°	-0.113	-0.0117	64.2	-22.8

Substitution of these values in (23) gives for $\beta = 0^\circ$

$$\frac{\bar{\dot{\psi}}'}{\bar{\delta}'} = \frac{-(22.8p + 1.307)}{p^2 + 0.0185p - 4.14} = \frac{-0.317\,(1 + 17.45p)}{(0.494p - 1)(0.489p + 1)} \qquad (24)$$

and for $\beta = 10^\circ$

$$\frac{\bar{\dot{\psi}}'}{\bar{\delta}'} = \frac{-(22.8p + 3.33)}{p^2 + 0.113p - 3.51} = \frac{-0.95\,(1 + 6.84p)}{(0.550p - 1)(0.518p + 1)}\,. \qquad (25)$$

Denoting the transfer function $\frac{\bar{\dot{\psi}}'}{\bar{\delta}'}$, by $-K_4G_4$ we have $K_4 = 0.317$ for zero incidence and 0.95 for 10° incidence. Equations (24) and (25) give the factors of the function G_4 for the two cases and Fig.18 shows the corresponding frequency response curves.

4.2 Frequency response study of control system with integral of error

Considering first the rate feedback loop, it can be seen from Fig.2 that the open loop transfer function is given by

$$\frac{\bar{e}_2'}{\bar{e}_3'} = \frac{\bar{e}_2'}{\bar{\dot{\psi}}'} \cdot \frac{\bar{\dot{\psi}}'}{\bar{\delta}'} \cdot \frac{\bar{\delta}'}{\bar{e}_3'} = K_2G_2K_3G_3K_4G_4 . \qquad (26)$$

The dashes indicate perturbations about steady values. Fig.19 shows the frequency response curves for $K_2G_2K_3G_3$ for a servo bandwidth of 5 c/s and the corresponding value of K_2K_3 (= 0.507) given for tanks full conditions in Table V of section 2. Only the 5 c/s case is examined in detail here to avoid complicating the diagrams. Fig.20 gives the frequency response curves corresponding to equation (26) for mean incidence values of 0° and 10° and Fig.21 shows the corresponding inner loop Nyquist diagrams.

It can be seen from Fig.20 that the phase margin is 61° at 1.86 c/s for both values of incidence and the gain margin 8.6 db at 4.56 c/s. Comparison with the corresponding figures for no aerodynamics given in Table I shows that the aerodynamic forces and moments have a negligible effect on the stability of the rate feedback loop. The transfer function $K_2G_2K_3G_3K_4G_4$ has a single pole in the right hand half of the p-plane arising from the unstable aerodynamic transfer function. Since the Nyquist diagram does not encircle the point (-1 + j0) the divergent instability is unaltered by the rate feedback loop and consequently the closed loop transfer function has a single pole in the right hand half of the p-plane.

The feedback transfer function of the outer loop is given by

$$\frac{\bar{\psi}'}{\bar{\psi}_c'} = \frac{K_5\left(1 + p\frac{K_1}{K_5}\right)}{p^2}\left[\frac{K_3G_3K_4G_4}{1 + K_2G_2K_3G_3K_4G_4}\right] . \qquad (27)$$

Fig.22 shows the frequency response curves of the function in square brackets, obtained from Fig.20 with the aid of a Nichols chart, and Fig.23 gives the curves corresponding to equation (27) for $K_1 = 1.84$ and $K_5 = 1.19$ (see Table VI). It can be seen from the latter figure that the phase margin is 57° at zero incidence and 59° at 10° incidence at 0.56 cycles per second, compared with 60° at 0.59 c/s in the absence of aerodynamic forces. The gain margin is 13.7 db at 2.66 c/s compared with 12.4 db at 2.42 c/s in the absence of aerodynamic forces.

The outer loop Nyquist diagram is shown in Fig.24. It is evident from the complete diagram (inset) that the contour makes one anti-clockwise and two clockwise (negative) encirclements of the point (-1 + j0) giving a net total of one negative encirclement (N = -1). Since the open loop transfer function has a single pole in the right hand half of the p-plane (P = 1) we have

$$\left.\begin{aligned} Z &= P + N \\ &= 0 \end{aligned}\right\} \qquad (28)$$

where Z denotes the number of zeros of the denominator of the closed loop transfer function. Hence the system is stable with the proposed values of loop gains.

It should be noted that if the outer loop gain were reduced by factors of 9.4 (19.5 db), at zero incidence, and 12.1 (21.7 db), at 10° incidence, the system would become unstable since there would then be one positive encirclement of the critical point and consequently Z would be equal to 2. Thus the system is conditionally stable in the presence of aerodynamic forces but, for the two cases considered, the gain margins in both directions are large.

4.3 Response to a step function change of demanded heading angle

It is of interest to compare the response, with and without aerodynamic forces, of the proposed system to a step change of heading angle demand. The calculations are simplified by neglecting, in both cases, the servo and rate gyroscope lags.

In the absence of aerodynamic forces the response of the integral of error system to a step function of magnitude ψ_D is given by

$$\bar{\psi} = \frac{(L_1L_2p + L_1L_6)\,\psi_D}{p\,(p^3 + L_1p^2 + L_1L_2p + L_1L_6)} \qquad (29)$$

where $L_1 = K_2K_3K_4$, $L_2 = \frac{K_1}{K_2}$ and $L_6 = \frac{K_5}{K_2}$.

It is assumed that all initial conditions are zero and that no limiting occurs. Similarly in the presence of aerodynamic forces

$$\bar{\psi}' = \frac{(L_1L_2p + L_1L_6)(n_\delta p + n_v y_\delta - y_v n_\delta)\,\psi_D'}{p\,[K_4p^2(p^2 - y_v p + Un_v) + (n_\delta p + n_v y_\delta - y_v n_\delta)(L_1p^2 + L_1L_2p + L_1L_6)]} \qquad (30)$$

where the dashes indicate that for non-linear aerodynamics the expression is only valid for small ψ_D.

With the gain parameters proposed for $f_3 = 3$, 5 and 10 c/s, given in Tables V and VI expression (29) gives

$$\psi = \psi_D\,[1 + 0.338e^{-0.508t} - 3.11e^{-3.29t}\sin(1.507t + 25.5^{\circ})] \quad \text{for } f_3 = 3 \text{ c/s}$$

$$\psi = \psi_D\,[1 + 0.341e^{-0.813t} - 3.31e^{-5.25t}\sin(2.23t + 23.9^{\circ})] \quad \text{for } f_3 = 5 \text{ c/s}$$

$$\psi = \psi_D\,[1 + 0.324e^{-1.37t} - 3.28e^{-9.29t}\sin(3.95t + 23.8^{\circ})] \quad \text{for } f_3 = 10 \text{ c/s}.$$

These expressions are plotted in Fig.25.

For the gain factors corresponding to $f_3 = 5$ c/s and for the aerodynamic parameters corresponding to zero and 10° incidence at U = 300 ft/sec, expression (30) gives

$$\psi' = \psi_D' [1 + 0.0228e^{-0.057t} + 0.0903e^{-0.988t} - 4.26e^{-4.53t} + 3.15e^{-6.10t}]$$

at zero incidence and

$$\psi' = \psi_D' [1 + 0.0693e^{-0.143t} - 0.0259e^{-0.975t} - 9.36e^{-5.29t} \sin(0.592t + 6.4^\circ]$$

at 10° incidence. These two expressions are illustrated in Fig.26.

It can be seen from Fig.25 that in the absence of aerodynamic forces the overshoot is approximately the same (about 15%) for the three servo bandwidths considered. This is in accordance with expectation since the loop gains were chosen to give a 60° phase margin in each case. The higher speeds of response obtainable with the larger loop gains is also evident. Comparison of Fig.26 with the corresponding curve ($f_3 = 5$ c/s) of Fig.25 indicates that the aerodynamic forces have the effect of reducing the overshoot and the speed of response. For instance, the time at which the heading angle passes the demanded value is increased from about 0.5 sec to about 0.9 sec and the peak overshoot is diminished from 15% to about 5%. The overshoot however decays more slowly the longest time constant being 1.2 sec in the absence of aerodynamics compared with 7 sec for $\beta = 10^\circ$ and 17.5 sec for zero incidence.

5 Conclusions

This preliminary design study has been made to determine suitable parameter values for two types of heading control system for RTV1. Linear servomechanism theory has been used throughout, the analysis being based on the assumption that the short period response of the system and its components can be represented approximately by linear transfer functions. The maximum values of the gain parameters, consistent with a well damped transient response, are tabulated in section 2 for the two types of system and for three possible rocket motor servo bandwidths. Adequate damping is ensured by choosing the values of loop gain to give a phase margin of 60° in both rate and position feedback loops.

Comparison of the responses of the two types of system to disturbances leads to the conclusion that the system including integral of error control is to be preferred. For example, it is shown that with the latter system a rocket motor bias results in a steady state component of velocity normal to the desired trajectory, assumed straight, whereas without integral of error a steady state normal acceleration component occurs.

A limited examination of the effects of aerodynamic forces and moments indicates that for the conditions assumed these will have little effect on the response of the proposed system. With an aerodynamically unstable configuration the system becomes conditionally stable, but it is shown that for the integral of error system, with the gain parameters proposed for a 5 c/s servo bandwidth, the gain margins in both directions are large. With the large stability margins proposed it appears to be unnecessary to make provision for varying the gain parameters in flight on account of aerodynamic forces or variations in the vehicle weight, moment of inertia etc. The combined effect of the latter is to alter the loop gains by about 1 db between tanks full and tanks empty conditions.

List of Symbols

Bar denotes Laplace Transform (e.g. $\bar{\delta}$)

Dot denotes differentiation with respect to time (e.g. $\dot{\psi}$)

Dash denotes perturbation quantity (e.g. v')

C	slug ft^2	Missile lateral moment of inertia
D_1	db	Gain of $\left(1 + p\frac{K_1}{K_5}\right)$ at frequency ω_c
D_2	db	Gain of $\frac{1}{p^2 G_2}\left[\frac{K_2G_2K_3G_3K_4G_4}{1 + K_2G_2K_3G_3K_4G_4}\right]$ at frequency ω_c
e_1	volts	Output from heading gyro pick-off
e_2	volts	Output from rate gyro pick-off
e_3	volts	Net input to rocket motor servo
f_2	cycles/sec	Undamped natural frequency of rate gyro
f_3	cycles/sec	Undamped natural frequency of rocket motor servo (servo bandwidth)
g	ft/sec^2	Acceleration due to gravity
G_2	-	Frequency variant part of rate gyro transfer function
G_3	-	Frequency variant part of rocket motor servo transfer function
G_4	-	Frequency variant part of missile transfer function
j	-	$\sqrt{-1}$
K_1	volts/degree	Heading gyro pick-off gain factor
K_2	volts/degree/sec	Rate gyro pick-off gain factor (invariant with frequency)
K_3	degrees/volt	Rocket motor servo gain factor (invariant with frequency)
K_4	sec^{-1}	Frequency invariant factor of missile transfer function
K_5	volts/sec/degree	Integrator gain factor
ℓ	ft	Distance between missile centre of gravity and rocket motor pivot point
L_1	-	Rate feedback loop gain $(= K_2K_3K_4)$
L_2	sec^{-1}	Position feedback loop gain $\left(= \frac{K_1}{K_2}\right)$
L_6	sec^{-2}	Integral of error loop gain $\left(= \frac{K_5}{K_2}\right)$

m	slugs	mass of missile
N	lb ft	Total moment in yaw plane
N_v	lb ft/ft/sec	Aerodynamic derivative $\frac{\partial N}{\partial v}$
N_r	lb ft/rad/sec	Aerodynamic derivative $\frac{\partial N}{\partial r}$
N_δ	lb ft/rad	Motor control derivative $\frac{\partial N}{\partial \delta}$
n_v	rad/sec^2/ft/sec	$\frac{N_v}{C}$
n_δ	sec^{-2}	$\frac{N_\delta}{C}$
N	[in eqn. (28) only]	Number of encirclements of the point (-1 + j0)
p	-	Laplace Transform variable
P	-	Number of poles of feedback transfer function in right hand half of the p-plane
r	degrees/sec or rad/sec	Rate of turn of missile ($= \dot{\psi}$)
t	sec	Time
t_1	sec	Time at which rocket motor moves from limit
T	lb	Rocket motor thrust
U	ft/sec	Missile flight path velocity
v	ft/sec	Missile side-slip velocity
x	ft	Displacement in a horizontal direction
y	ft	Displacement in a vertical direction
Y	lb	Total normal force in yaw plane
Y_v, Y_r and Y_δ	-	Aerodynamic and control derivatives $\frac{\partial Y}{\partial v}$, $\frac{\partial Y}{\partial r}$ and $\frac{\partial Y}{\partial \delta}$ respectively
y_v and y_δ	-	$\frac{Y_v}{m}$ and $\frac{Y_\delta}{m}$ respectively
Z	-	Number of zeros of denominator of closed loop transfer function
β	degrees or radians	Missile angle of incidence
δ	degrees or radians	Rocket motor deflection with respect to missile longitudinal axis
δ_1	degrees	Rocket motor deflection bias

Δ	degrees	Limit of rocket motor deflection
ζ_2		Rate gyro damping factor
ζ_3		Servo damping factor
ϕ_1	degrees	Phase of the term $\left(1 + p\frac{K_1}{K_5}\right)$ at frequency ω_c
ϕ_2	degrees	Phase of the term $\frac{1}{p^2 G_2}\left[\frac{K_2G_2K_3G_3K_4G_4}{1 + K_2G_2K_3G_3K_4G_4}\right]$ at frequency ω_c
ψ	degrees	Heading angle of missile with respect to vertical datum
ψ_D	degrees	Demanded heading angle (gyro datum) with respect to vertical datum
ψ_ε	degrees	Heading angle error with respect to gyro datum ($= \psi_D - \psi$)
ω_o	rad/sec	Break frequency of the term $\left(1 + p\frac{K_1}{K_5}\right)$ (see Fig.9)
ω_c	rad/sec	Angular frequency at which feedback gain is unity (cut-off frequency)
ω_2	rad/sec	$2\pi f_2$
ω_3	rad/sec	$2\pi f_3$

REFERENCES

No.	Author	Title, etc
1	A.P. MacLaren	A Preliminary Assessment of the Problems Associated with the Control of Medium Range Ballistic Rockets. RAE Tech Note GW 339.
2	G.T. Eynon	Development of a Hydraulic Servo for Angular Position Control of the RTV1 Combustion Chamber. RAE Tech Note GW 368.

Attached:- Appendix I
Drgs. GW/P/6926 to 6950
Detachable Abstract Cards

Advance Distribution

Ministry of Supply		R.A.E.			
Chief Scientist		Director	Aero	2	GWTW
CGWL		DD(E)	Structures	2	Patents
DG/GW	80	DD(A)	IAP	3	NAE Library
RRE (Mr. C.P.Fogg)	4	RPD 3	GWTD		Library
TPA3/TIB	90				

APPENDIX I

Details of Trajectory Calculations

The following calculations of approximate trajectories are based on the assumptions set out in section 3 and the equations given in section 3.1. The gain parameters are given in Tables IV, V and VI.

1. Deviation due to a 3° Initial Heading Angle Error

(a) Control system of Fig.1 (without integral of error)

The control equation for this case, from equation (16), is

$$\delta = K_1K_3\psi + K_2K_3\dot{\psi} . \qquad (I.1)$$

The assumed initial conditions are $\psi_o = 3^\circ$ and $\dot{\psi} = 0$ giving $\delta_o = 3K_1K_3$ degrees. It can be seen from Table V that for $f_3 = 3$, 5 and 10 cycles per second, $3K_1K_3 = 3.39^\circ$, 8.37° and 25.92° respectively. Thus the initial value of demanded motor deflection, for $f_3 = 5$ and 10 c/s, exceeds the assumed 5° limit, and so the actual deflection will remain constant at the limit value for a short period at the beginning of flight. Referring to equation (13), it is evident that the missile angular motion during this period is given by

$$\ddot{\psi} = -\frac{T\ell}{C}\Delta = -K_4\Delta \qquad (I.2)$$

where Δ denotes the limit value of motor deflection. Hence

$$\dot{\psi} = -K_4\Delta t \qquad (I.3)$$

and

$$\psi = \psi_o - \tfrac{1}{2}K_4\Delta t^2 . \qquad (I.4)$$

The time t_1 at which the demanded motor deflection falls to Δ may be obtained by substituting expressions (I.3) and (I.4) in the control equation (I.1) and solving for t. Hence

$$t_1 = -\frac{1}{L_2} \pm \sqrt{\left(\frac{1}{L_2}\right)^2 + 2\left(\frac{\psi_o}{K_4\Delta} - \frac{1}{L_1L_2}\right)} \qquad (I.5)$$

where, as before, $L_1 = K_2K_3K_4$ and $L_2 = \frac{K_1}{K_2}$ and only real and positive values of t_1 are admissible.

The trajectory during the period 0 to t_1 is obtained from

$$\ddot{x} = \frac{T}{m}(\psi + \Delta) \qquad (I.6)$$

and

$$\ddot{y} = \frac{T}{m} - g \qquad (I.7)$$

whence the displacement (x_1, y_1) at time t_1 is given by

$$x_1 = \frac{T}{m}\left[\frac{1}{2}(\psi_o + \Delta)t_1^2 - \frac{1}{24}K_4\Delta t_1^4\right] \qquad (I.8)$$

and

$$y_1 = \frac{1}{2}\left(\frac{T}{m} - g\right)t_1^2 \ . \qquad (I.9)$$

The corresponding values of ψ_1 and $\dot{\psi}_1$ are obtained from expressions (I.3) and (I.4). Table VIII gives the conditions at time t_1 for the three cases with the gain parameters specified in Table V.

Table VIII

Conditions at time t_1

Servo bandwidth f_3 c/s	t_1 sec	x_1 ft	y_1 ft	$\dot{x}_1$ ft/sec	$\dot{y}_1$ ft/sec	ψ_1 degrees	$\dot{\psi}_1$ deg/sec	δ_1 degrees
3	0	0	0	0	0	3.0	0	3.39
5	0.0529	0.0111	0.0345	0.417	1.30	2.85	-5.87	5.0
10	0.129	0.0648	0.205	0.984	3.17	2.08	-14.30	5.0

After time t_1 the trajectory is obtained by solving equations (13), (16), (18) and (19) with the initial conditions given in Table VIII. Transformation of equation (13) gives

$$p^2\bar{\psi} = -K_4\bar{\delta} + \dot{\psi}_1 + p\psi_1 \qquad (I.10)$$

where, as before, the bar notation indicates Laplace Transforms. Similarly, equation (16) becomes

$$\bar{\delta} = K_1K_3\ddot{\psi} + K_2K_3(p\bar{\psi} - \psi_1) \ . \qquad (I.11)$$

Solution of equations (I.10) and (I.11) gives

$$\bar{\psi} = \frac{(p+L_1)\psi_1 + \dot{\psi}_1}{p^2 + L_1p + L_1L_2} \qquad (I.12)$$

and

$$\bar{\delta} = \frac{L_1L_2\psi_1 p + L_1\dot{\psi}_1(p+L_2)}{K_4(p^2+L_1p+L_1L_2)} \ . \qquad (I.13)$$

From equation (18) we have

$$p^2\bar{x} = \frac{T}{m}(\bar{\psi}+\bar{\delta}) + \dot{x}_1 + px_1 \qquad (I.14)$$

and substitution of expressions (I.12) and (I.13) in (I.14) gives

$$\bar{x} = \frac{T\{p(K_4\psi_1+L_1L_2\psi_1+L_1\dot{\psi}_1) + K_4L_1\psi_1 + (K_4+L_1L_2)\dot{\psi}_1\}}{m\,p^2\,K_4(p^2+L_1p+L_1L_2)} + \frac{\dot{x}_1}{p^2} + \frac{x_1}{p} . \qquad (I.15)$$

Finally, from equation (19), we obtain

$$\bar{y} = \left(\frac{T}{m} - g\right)\frac{1}{p^3} + \frac{\dot{y}_1}{p^2} + \frac{y_1}{p} . \qquad (I.16)$$

The missile motion after t_1, in terms of ψ, δ, x and y as functions of time, is obtained from the inverse transformations of expressions (I.12), (I.13), (I.15) and (I.16). These functions are given in Table IX and Fig.14 shows the corresponding trajectories. In this table t denotes time after t_1.

Table IX

Motion after time t_1

f_3	ψ degrees	δ degrees
3 c/s	$4.23e^{-3.54t}\cos(3.57t-0.782)$	$4.81e^{-3.54t}\cos(3.57t+0.778)$
5 c/s	$3.49e^{-5.65t}\cos(5.51t-0.476)$	$9.55e^{-5.65t}\cos(5.51t+1.019)$
10 c/s	$2.18e^{-9.975t}\cos(9.54t-0.304)$	$18.8e^{-9.975t}\cos(9.54t+1.305)$
f_3	x feet	y feet
3 c/s	$0.0182 + 0.834t -$ $e^{-3.54t}(0.0182\cos 3.57t + 0.252\sin 3.57t)$	$12.3t^2$
5 c/s	$0.1077 + 0.573t -$ $e^{-5.65t}(0.0966\cos 5.51t + 0.127\sin 5.51t)$	$0.0305 + 1.30t + 12.3t^2$
10 c/s	$0.1538 + 0.486t -$ $e^{-9.975t}(0.089\cos 9.54t + 0.0407\sin 9.54t)$	$0.205 + 3.17t + 12.3t^2$

(b) Control system of Fig.2 (with integral of error)

It can be seen from Table VI that in this case also a 3° initial heading error demands an initial motor deflection greater than 5° for the gain parameters corresponding to $f_3 = 5$ and 10 cycles per second. Hence for these two cases the angular motion during the launching phase is again given by equation (I.2), (I.3) and (I.4). In addition we have

$$\int \psi\,dt = \psi_0 t - \frac{1}{6}K_4\Delta t^3 \qquad (I.17)$$

assuming that the integrator output is held at zero until the instant of launch ($t = 0$).

Substitution of expressions (I.3), (I.4) and (I.17) in (17), the control equation for this case, gives the following equation for t_1, the time at which the demanded motor deflection falls to Δ:

$$t^3 + \frac{3}{L_5} t^2 + 6\left(\frac{1}{L_6} - \frac{\psi_o}{K_4\Delta}\right) t + 6\left(\frac{1}{L_1 L_6} - \frac{\psi_o}{K_4 L_5 \Delta}\right) = 0. \qquad (I.18)$$

where $L_1 = K_2K_3K_4$, $L_5 = \frac{K_5}{K_1}$ and $L_6 = \frac{K_5}{K_2}$.

The required value of t_1 is given by the smallest real and positive root of equation (I.18) and the displacement at this time is obtained from expressions (I.8) and (I.9). Table X gives the conditions at t_1 for the three cases.

Table X

Conditions at time t_1

Servo bandwidth f_3 c/s	t_1 sec	x_1 ft	y_1 ft	$\dot{x}_1$ ft/sec	$\dot{y}_1$ ft/sec	ψ_1 degrees	$\dot{\psi}_1$ deg/sec	δ_1 degrees
3	0	0	0	0	0	3.0	0	2.21
5	0.0102	0.0002	0.0013	0.035	0.251	2.99	-1.13	5.0
10	0.1057	0.019	0.137	0.354	2.60	2.38	-11.75	5.0

After time t_1 the missile trajectory is obtained from the solution of equations (13), (17), (18) and (19) with the initial conditions given in Table X. Differentiating and transforming equation (17) gives

$$p\bar{\delta} - \delta_1 = K_5K_3\bar{\psi} + K_1K_3(p\bar{\psi} - \psi_1) + K_2K_3(p^2\bar{\psi} - \dot{\psi}_1 - p\psi_1) \qquad (I.19)$$

and solving (I.19) with (I.10) gives

$$\bar{\psi} = \frac{\psi_1(p^2 + L_1p + L_1L_2) + \dot{\psi}_1(p + L_1) - K_4\delta_1}{p^3 + L_1p^2 + L_1L_2p + L_1L_6} \qquad (I.20)$$

and

$$\bar{\delta} = \frac{L_1L_6\left[p\psi_1 + \dot{\psi}_1\left(\frac{p}{L_5} + 1\right)\right] + p^2K_4\delta_1}{K_4(p^3 + L_1p^2 + L_1L_2p + L_1L_6)}. \qquad (I.21)$$

Substitution of expressions (I.20) and (I.21) in (I.14) gives

$$\bar{x} = \frac{T\left\{\psi_1\left[p^2 + L_1p\left(1 + \frac{L_6}{K_4}\right) + L_1L_2\right] + \dot{\psi}_1\left[p\left(1 + \frac{L_1L_2}{K_4}\right) + L_1\left(1 + \frac{L_6}{K_4}\right)\right] + \delta_1(p^2 - K_4)\right\}}{mp^2(p^3 + L_1p^2 + L_1L_2p + L_1L_6)}$$

$$+ \frac{x_1}{p} + \frac{\dot{x}_1}{p^2} \qquad (I.22)$$

and $\bar{y}$ is again given by expression (I.16).

The motion after time t_1, in terms of ψ, δ, x and y as functions of time, is derived from the above equations. These functions are given in Table XI, in which t denotes time after t_1, and Fig.15 shows the corresponding trajectories.

Table XI

Motion after time t_1

f_3 c/s	ψ degrees	δ degrees
3	$e^{-3.285t}$ (4.01 cos 1.507t + 8.42 sin 1.507t) − 1.01$e^{-0.508t}$	$e^{-3.285t}$ (2.21 cos 1.507t − 5.02 sin 1.507t) + 0.012$e^{-0.508t}$
5	$e^{-5.245t}$ (4.00 cos 2.236t + 8.14 sin 2.236t) − 1.00$e^{-0.813t}$	$e^{-5.245t}$ (4.95 cos 2.236t − 13.24 sin 2.236t) + 0.05$e^{-0.813t}$
10	$e^{-9.29t}$ (2.95 cos 3.95t − 3.89 sin 3.95t) − 0.57$e^{-1.37t}$	$e^{-9.29t}$ (4.90 cos 3.95t − 27.1 sin 3.95t) + 0.10$e^{-1.37t}$
f_3 c/s	x feet	y feet
3	3.32 − 3.82$e^{-0.508t}$ + a damped oscillatory term	$12.3t^2$
5	1.36 − 0.047t − 1.43$e^{-0.813t}$ + a damped oscillatory term	$0.0013 + 0.251t + 12.3t^2$
10	0.43 − 0.46t − 0.25$e^{-1.37t}$ + a damped oscillatory term	$0.137 + 2.60t + 12.3t^2$

The damped oscillatory transient term of x is not given in detail in the above table as it becomes negligible after one second.

2. Deviation due to a 1° Motor Deflection Bias

(a) Control system of Fig.1 (without integral of error)

In this case it is assumed that a constant bias exists in the control system, such that the actual rocket motor deflection is given by

$$\delta = K_1K_3\psi + K_2K_3\dot{\psi} - \delta_1 \qquad (I.23)$$

instead of by equation (16). No limiting occurs in this case since no initial heading error is assumed and the bias δ_1 is assumed equal to 1°. Transformation of equation (I.23) gives

$$\bar{\delta} = K_1K_3\bar{\psi} + K_2K_3p\bar{\psi} - \frac{\delta_1}{p} \qquad (I.24)$$

and from equation (13) we have

$$p^2\bar{\psi} = -K_4\bar{\delta} \qquad \text{(I.25)}$$

whence

$$\bar{\psi} = \frac{K_4\,\delta_1}{p(p^2 + L_1p + L_1L_2)} \qquad \text{(I.26)}$$

and

$$\bar{\delta} = \frac{-p\,\delta_1}{p^2 + L_1p + L_1L_2}\,. \qquad \text{(I.27)}$$

Transforming equations (18) and (19) and substituting gives

$$\bar{x} = \frac{T(K_4 - p^2)\,\delta_1}{mp^3(p^2 + L_1p + L_1L_2)} \qquad \text{(I.28)}$$

and

$$\bar{y} = \frac{T - mg}{mp^3}\,. \qquad \text{(I.29)}$$

The trajectories obtained by transforming equations (I.28) and (I.29) into functions of time are shown in Fig.16 for the three sets of parameters corresponding to $f_3 = 3$, 5 and 10 cycles per second. Table XII gives ψ, δ, x and y as functions of time for the three cases.

Table XII

Motion due to 1° bias

f_3 c/s	ψ degrees	δ degrees
3	$0.88\,[1 - e^{-3.54t}\,(\cos 3.57t + 0.992 \sin 3.57t)]$	$e^{-3.54t}\,(0.992 \sin 3.57t - \cos 3.57t)$
5	$0.36\,[1 - e^{-5.65t}\,(\cos 5.51t + 1.025 \sin 5.51t)]$	$e^{-5.65t}\,(1.025 \sin 5.51t - \cos 5.51t)$
10	$0.116\,[1 - e^{-9.975t}\,(\cos 9.54t + 1.045 \sin 9.54t)]$	$e^{-9.975t}\,(1.045 \sin 9.54t - \cos 9.54t)$
f_3 c/s	x feet	y feet
3	$0.435t^2 - 0.244t - 0.0054$ + a damped oscillatory term	$12.3t^2$
5	$0.1765t^2 - 0.064t - 0.010$ + a damped oscillatory term	$12.3t^2$
10	$0.0575t^2 - 0.012t - 0.0045$ + a damped oscillatory term	$12.3t^2$

(b) Control system of Fig.2 (with integral of error)

It is assumed in this case that the rocket motor deflection is given by

$$\delta = K_5K_3 \int \psi dt + K_1K_3\psi + K_2K_3\dot{\psi} - \delta_i \qquad (I.30)$$

instead of by equation (17). Again no limiting occurs as all initial conditions are assumed to be zero and δ_i is assumed equal to one degree. The following expressions for the Laplace transforms of ψ, δ and x are obtained from equations (13), (18) and (I.30):-

$$\bar{\psi} = \frac{K_4\,\delta_i}{p^3 + L_1p^2 + L_1L_2p + L_1L_6} \qquad (I.31)$$

$$\bar{\delta} = \frac{-p^2\,\delta_i}{p^3 + L_1p^2 + L_1L_2p + L_1L_6} \qquad (I.32)$$

and

$$\bar{x} = \frac{T(K_4 - p^2)\,i}{mp^2(p^3 + L_1p^2 + L_1L_2p + L_1L_6)} \,. \qquad (I.33)$$

$\bar{y}$ is again given by expression (I.29).

The trajectories obtained from equations (I.29) and (I.33) are shown in Fig.17 and Table XIII gives x and y as functions of time for the three cases.

Table XIII

Motion due to 1° bias

f_3 c/s	x feet	y feet
3	$-8.2 + 3.30t + 8.4e^{-0.508t}$ + a damped oscillatory term	$12.3t^2$
5	$-1.29 + 0.83t + 1.31e^{-0.813t}$ + a damped oscillatory term	$12.3t^2$
10	$-0.143 + 0.157t + 0.137e^{-1.37t}$ + a damped oscillatory term	$12.3t^2$

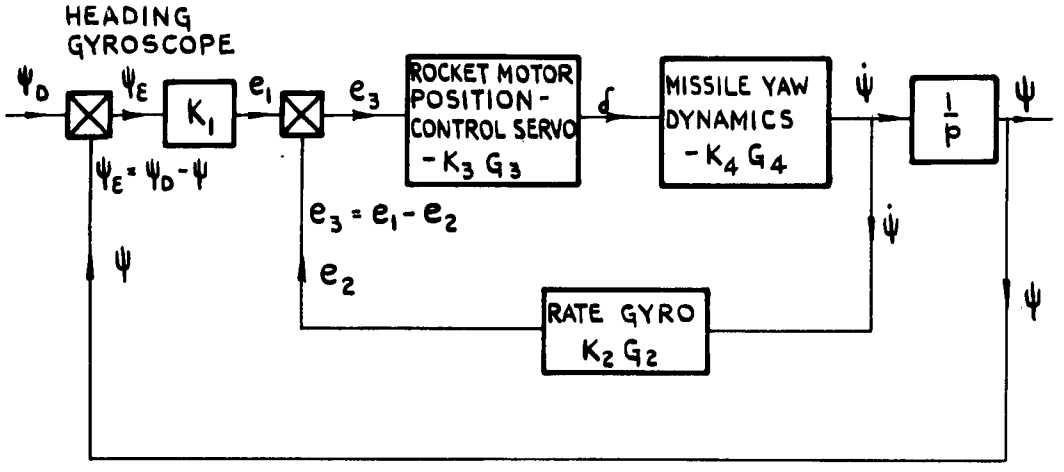

FIG.I. BLOCK DIAGRAM OF CONTROL SYSTEM USING HEADING ANGLE ERROR AND RATE FEEDBACK.

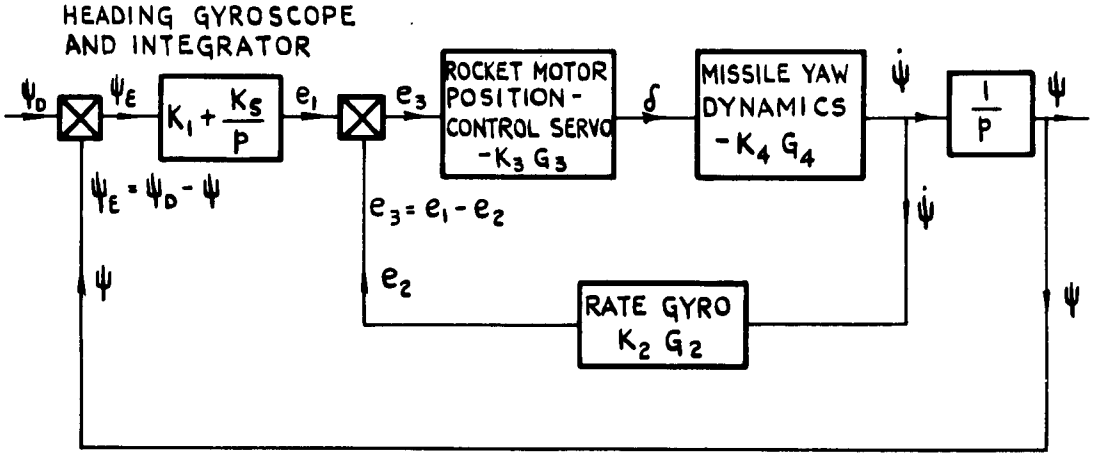

FIG.2. BLOCK DIAGRAM OF CONTROL SYSTEM USING HEADING ANGLE ERROR, INTEGRAL OF ERROR AND RATE FEEDBACK.

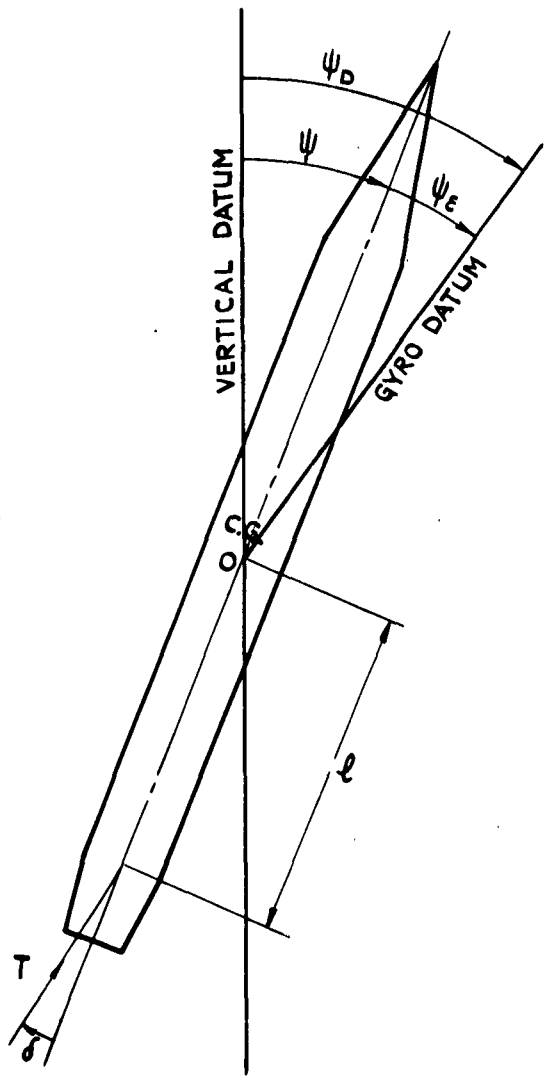

FIG. 3. CONVENTION FOR MISSILE DYNAMICS IN YAW NEGLECTING AERODYNAMICS.

(ANGLES SHOWN POSITIVE)

FIG.4.

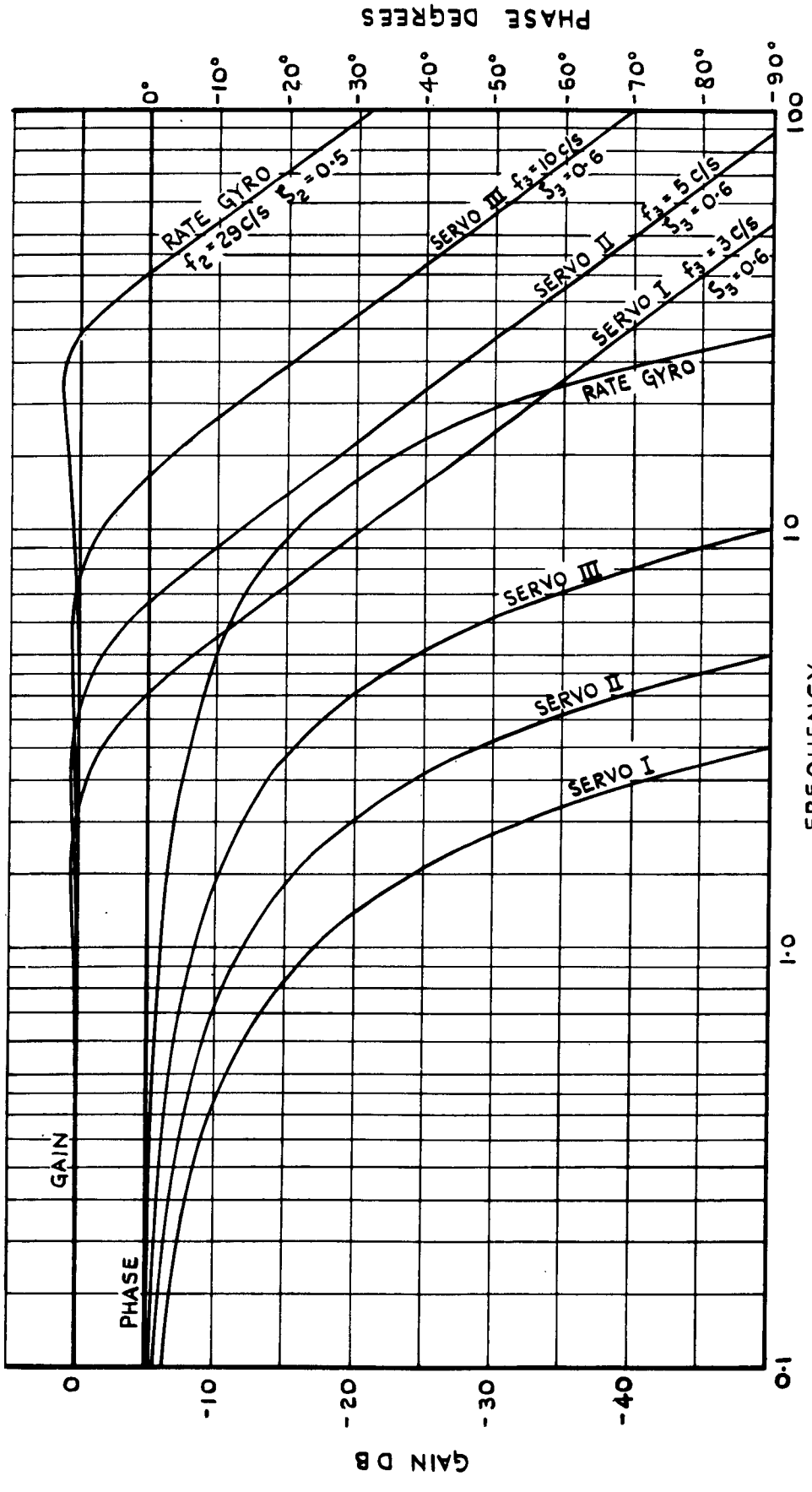

FIG.4. FREQUENCY RESPONSE CURVES FOR ASSUMED SERVOS AND RATE GYRO.

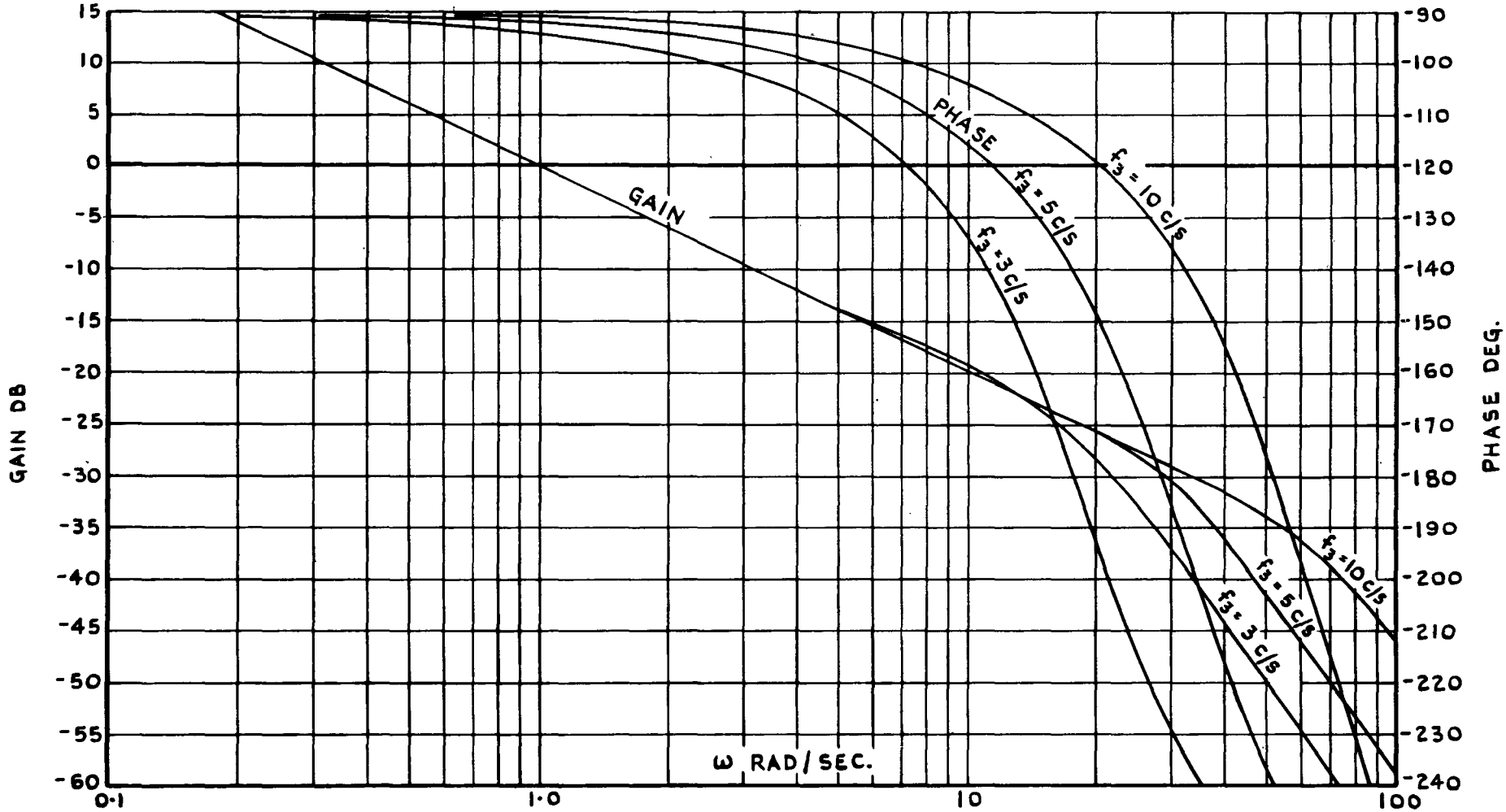

FIG. 5. RESPONSE OF FREQUENCY VARIANT G_2 G_3 G_4 FOR THE RATE FEEDBACK LOOP.

FIG. 5.

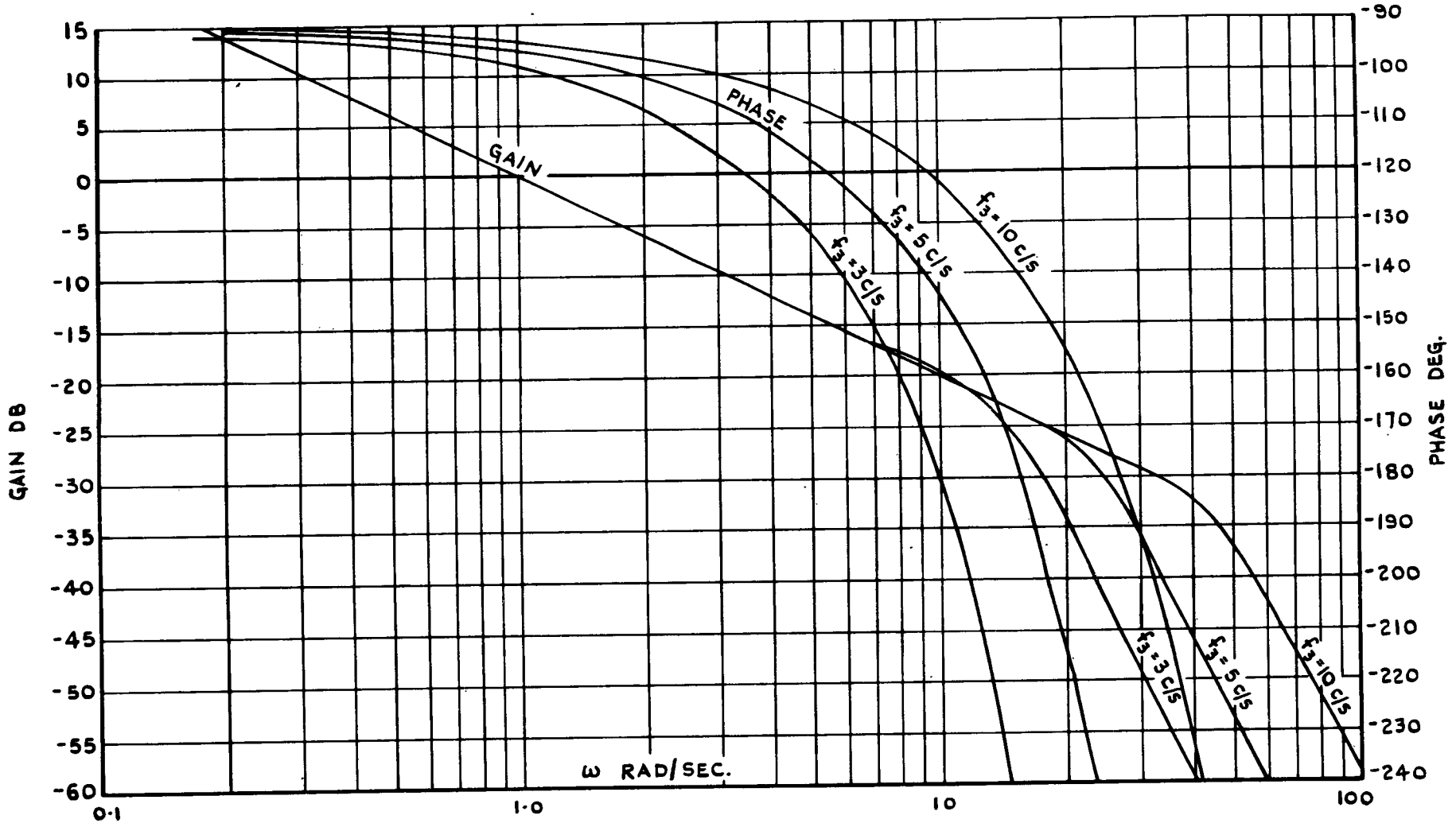

FIG. 6. RESPONSE OF $\frac{1}{G_2 P}\left[\frac{K_2 G_2 K_3 G_3 K_4 G_4}{1 + K_2 G_2 K_3 G_3 K_4 G_4}\right]$ FOR THE OUTER LOOP OF THE CONTROL SYSTEM IN FIG. 1.

T.N. GW. 397.
FIG. 6.

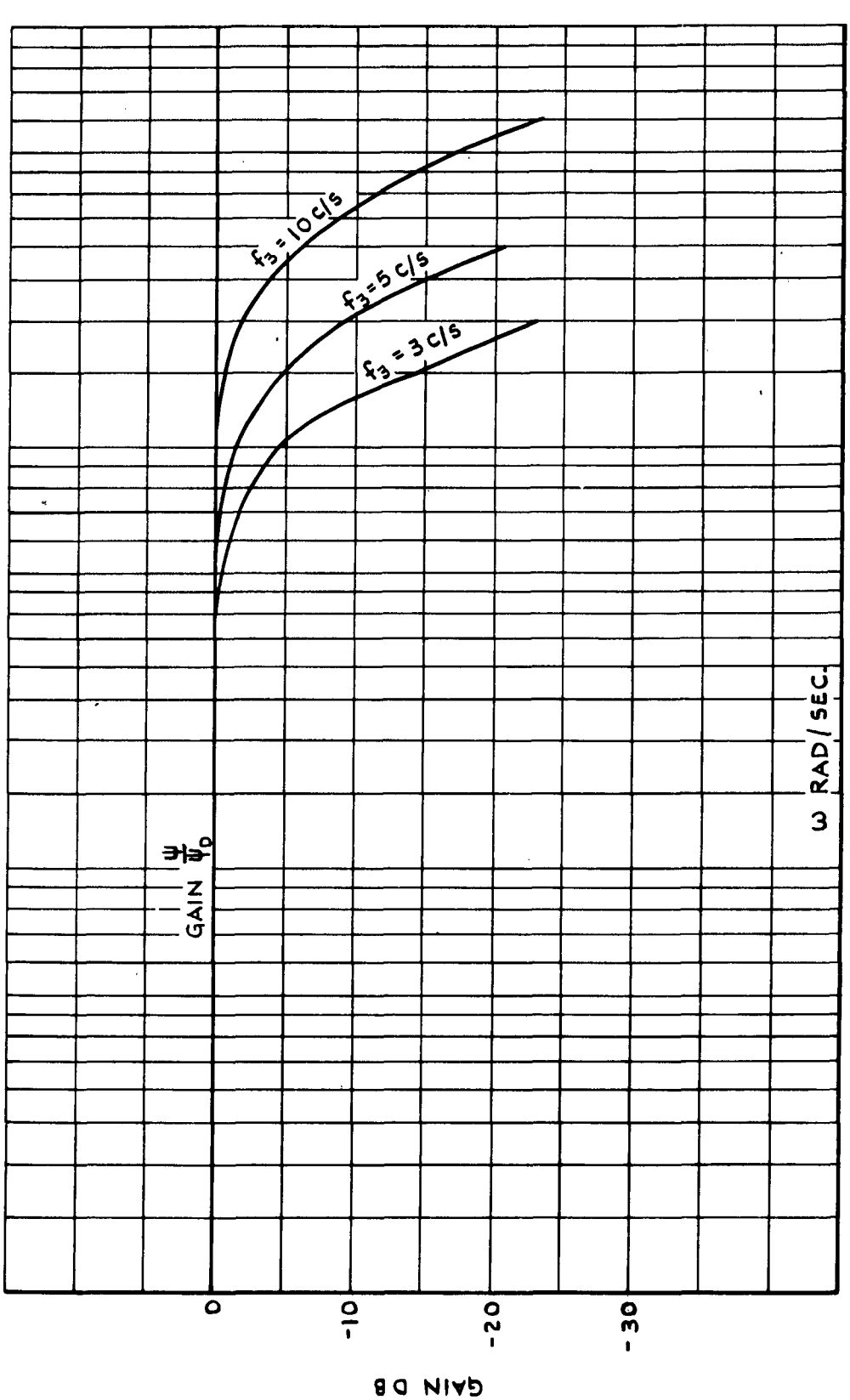

FIG. 7. CLOSED LOOP RESPONSE FOR THE OUTER LOOP OF THE CONTROL SYSTEM IN FIG. 1.

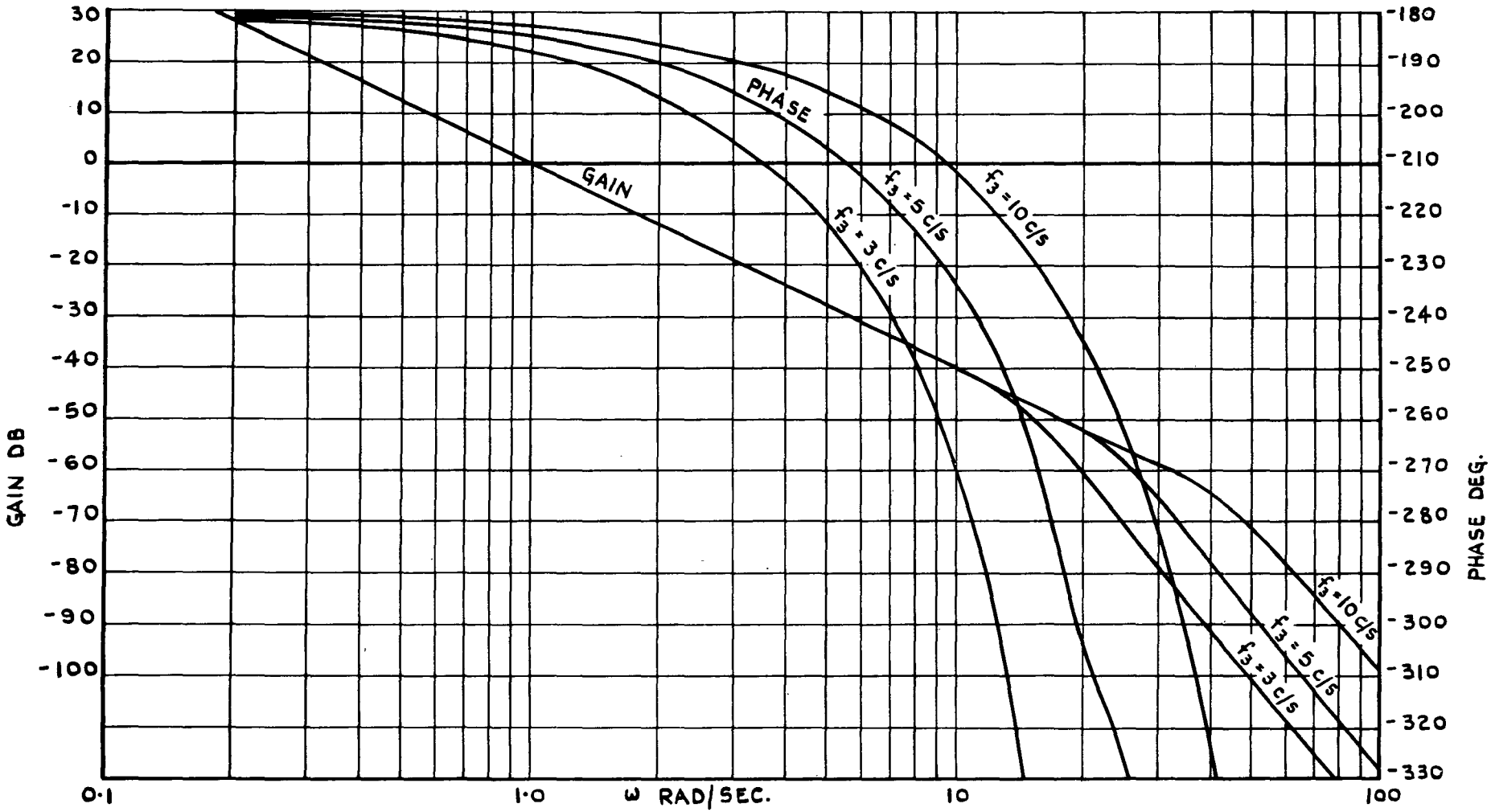

FIG. 8. RESPONSE OF $\frac{1}{G_2 p^2}\left[\frac{K_2G_2K_3G_3K_4G_4}{1+K_2G_2K_3G_3K_4G_4}\right]$ FOR THE OUTER LOOP OF THE CONTROL SYSTEM IN FIG. 2.

FIG. 9.

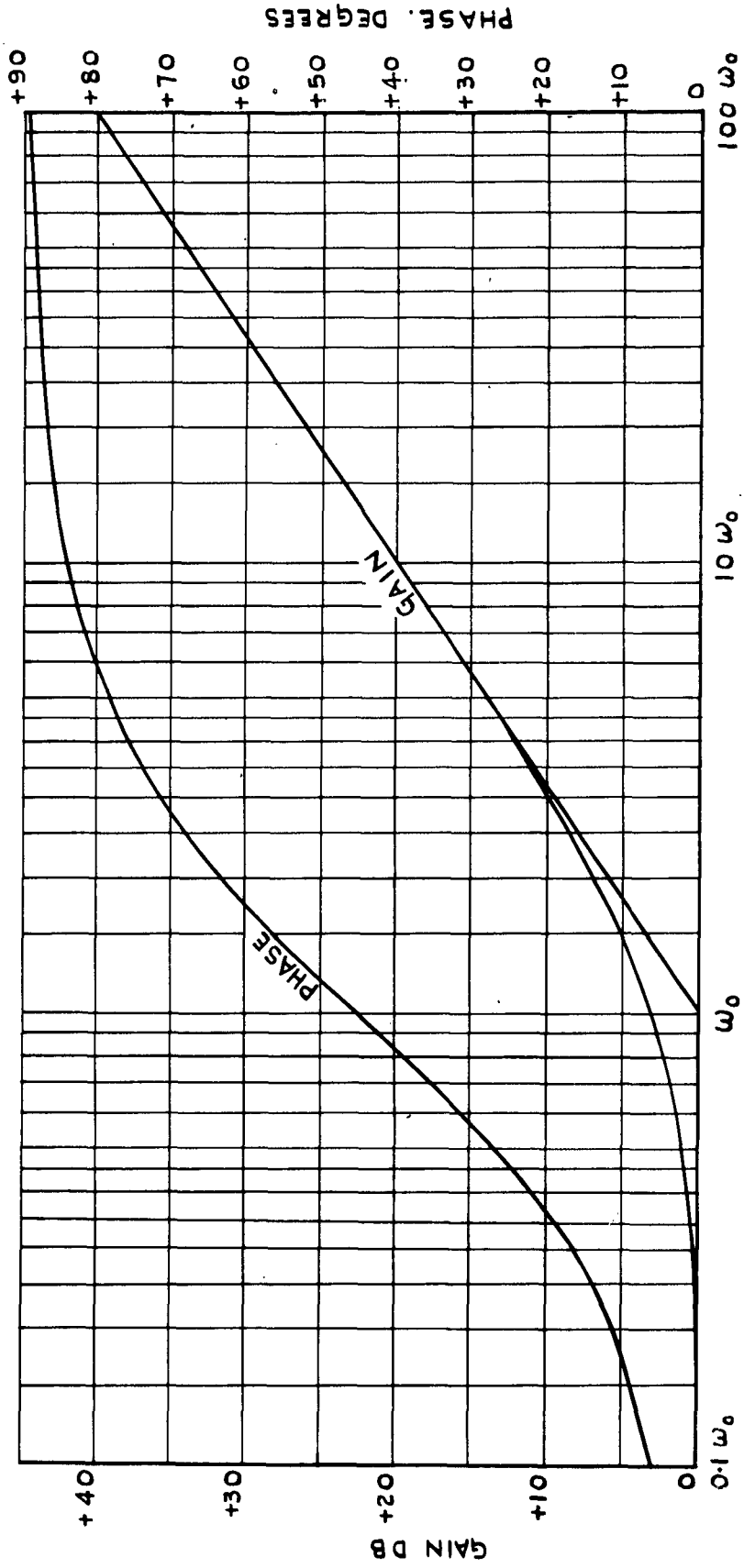

FIG. 9. FREQUENCY RESPONSE CURVES FOR THE FUNCTION $\left(1 + \frac{p}{\omega_0}\right)$

FIG.10.

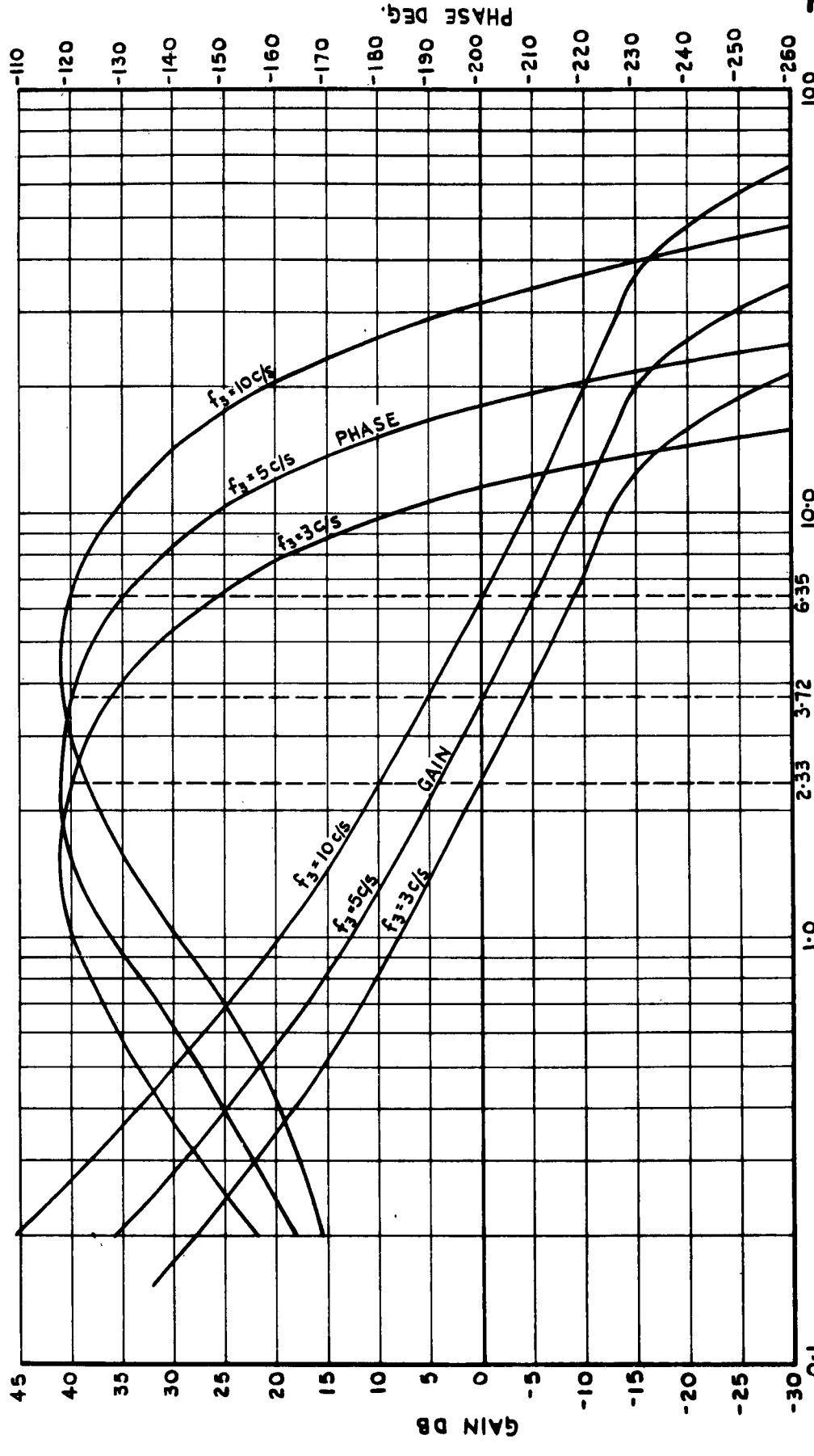

FIG.10. RESPONSE FOR $\phi_1 = 80^\circ$ OF $\frac{K_3}{K_2}\frac{(1+P\frac{K_1}{K_2})}{G_2 P^2}\left[\frac{K_2 G_2 K_3 G_3 K_4 G_4}{1+K_2 G_2 K_3 G_3 K_4 G_4}\right]$ FOR THE OUTER LOOP OF THE CONTROL SYSTEM IN FIG. 2.

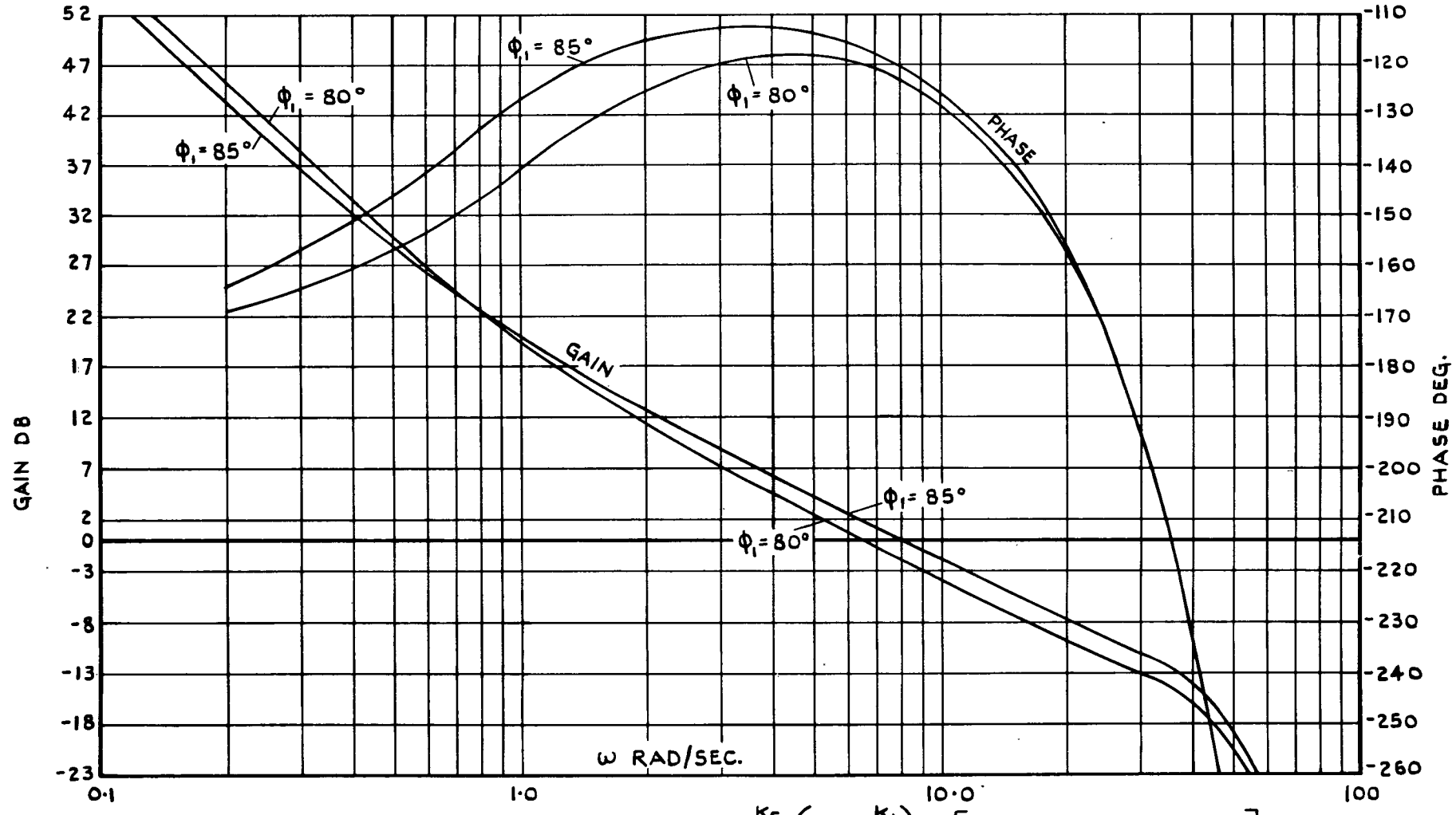

FIG.11. COMPARISON OF RESPONSE OF $\frac{\frac{K_5}{K_2}\left(1+p\,\frac{K_1}{K_5}\right)}{G_2\,p^2}\left[\frac{K_2\,G_2\,K_3\,G_3\,K_4\,G_4}{1+K_2\,G_2\,K_3\,G_3\,K_4\,G_4}\right]$ FOR $\phi_1 = 80°$ AND $\phi_1 = 85°$ WITH $f_3 = 10$ CYCLES PER SEC.

6935

T.N.G.W.397.
FIG.11.

FIG.12.

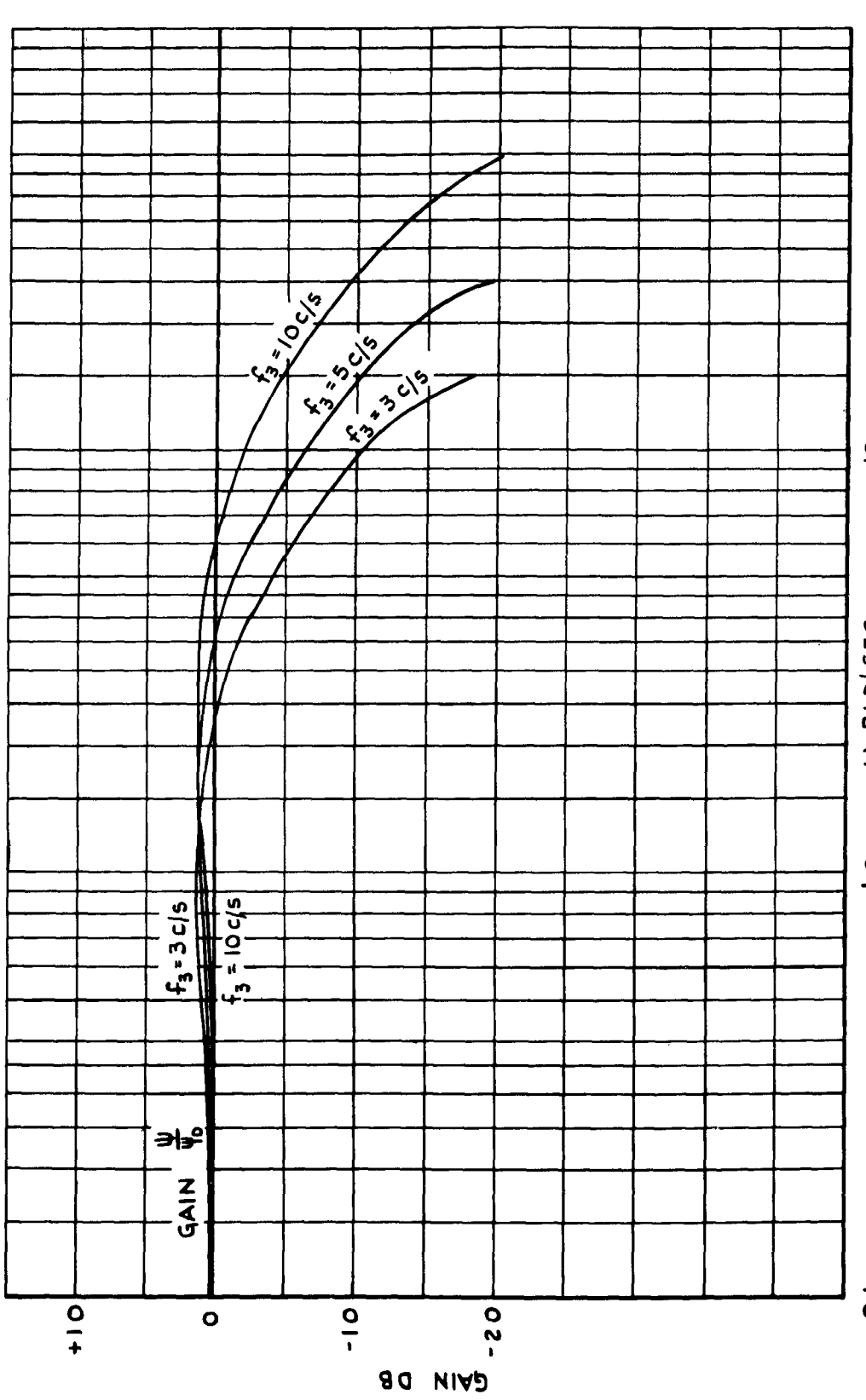

FIG. 12. CLOSED LOOP RESPONSE FOR THE OUTER LOOP OF THE CONTROL SYSTEM IN FIG. 2.

CURVE I ⊙ WITHOUT INTEGRAL OF ERROR
CURVE II ⊡ WITH INTEGRAL OF ERROR
f_s = 10 CYCLES PER SEC. IN BOTH CASES
FREQUENCIES IN RADIANS PER SECOND

INSE

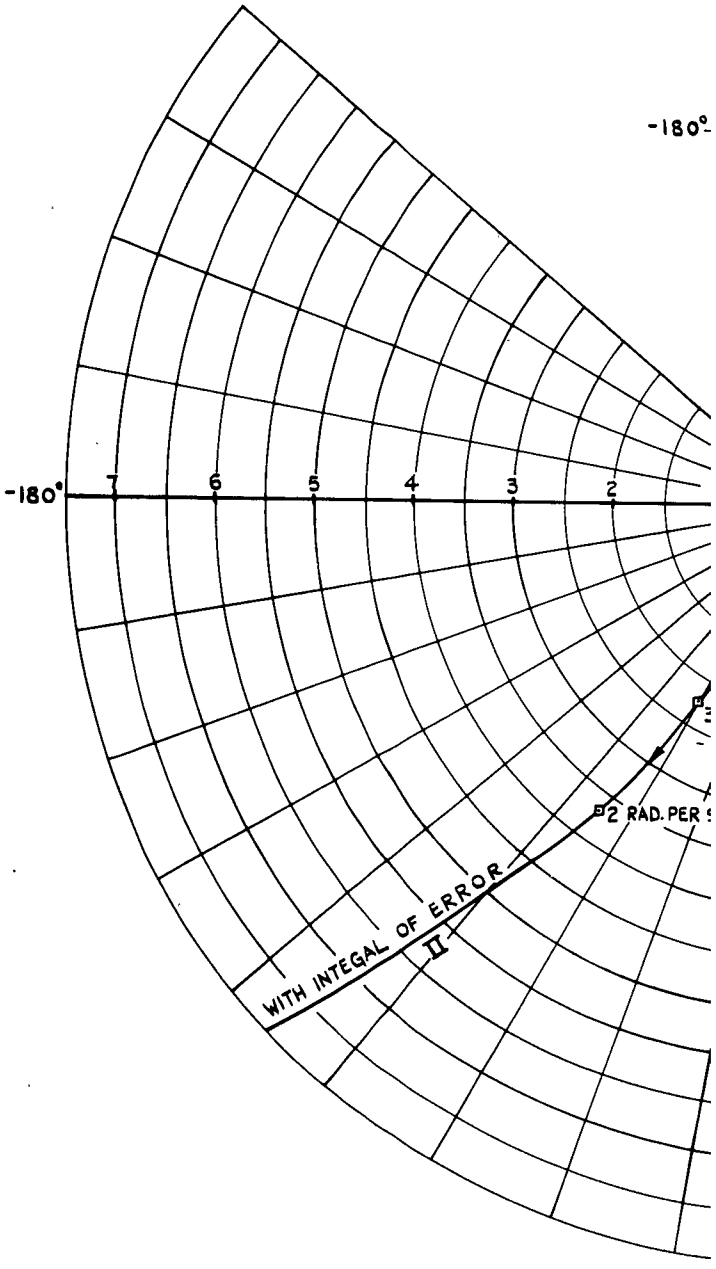

FIG.13. POLAR PLOTS OF FEEDB

PROPOSED TYP

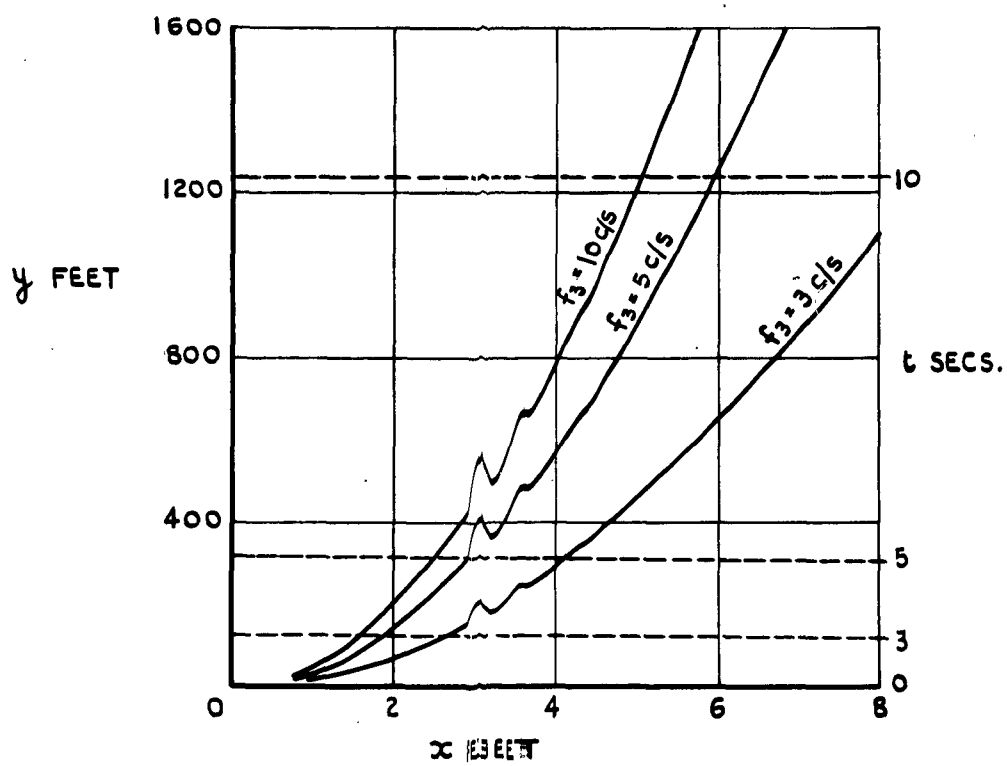

f_3 = SERVO BANDWIDTH

FIG.14. MISSILE TRAJECTORIES RESULTING FROM A 3° INITIAL HEADING ANGLE ERROR FOR THE CONTROL SYSTEM OF FIG.1. (WITHOUT INTEGRAL OF ERROR).

FIG .15.

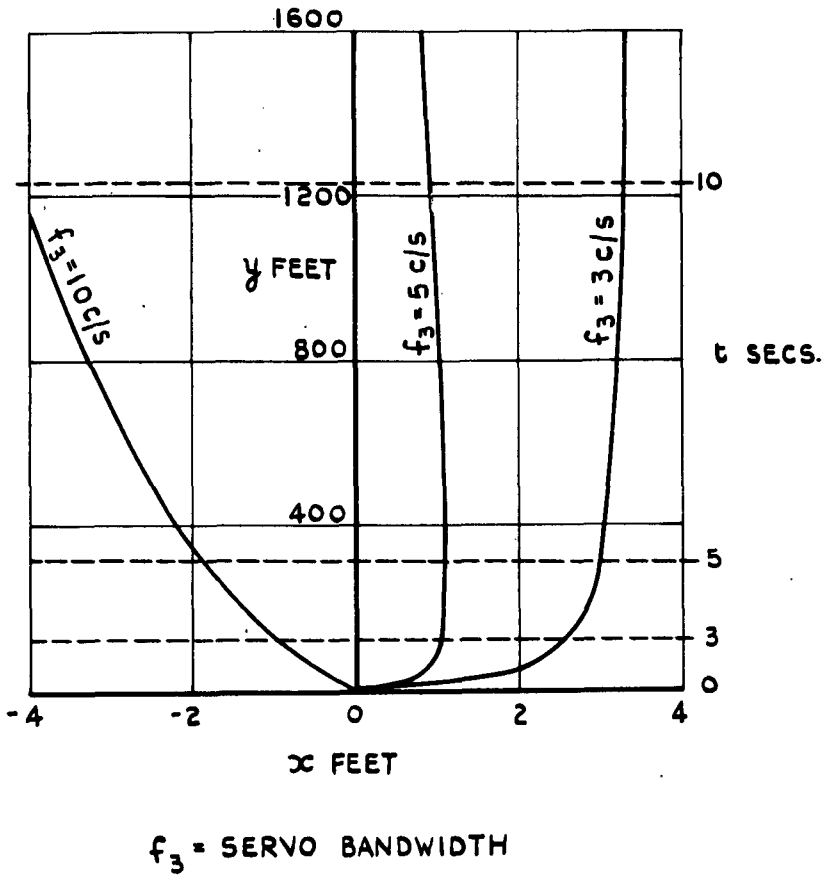

FIG.15. MISSILE TRAJECTORIES RESULTING FROM A 3° INITIAL HEADING ANGLE ERROR FOR THE CONTROL SYSTEM OF FIG.2. (WITH INTEGRAL OF ERROR).

FIG.16.

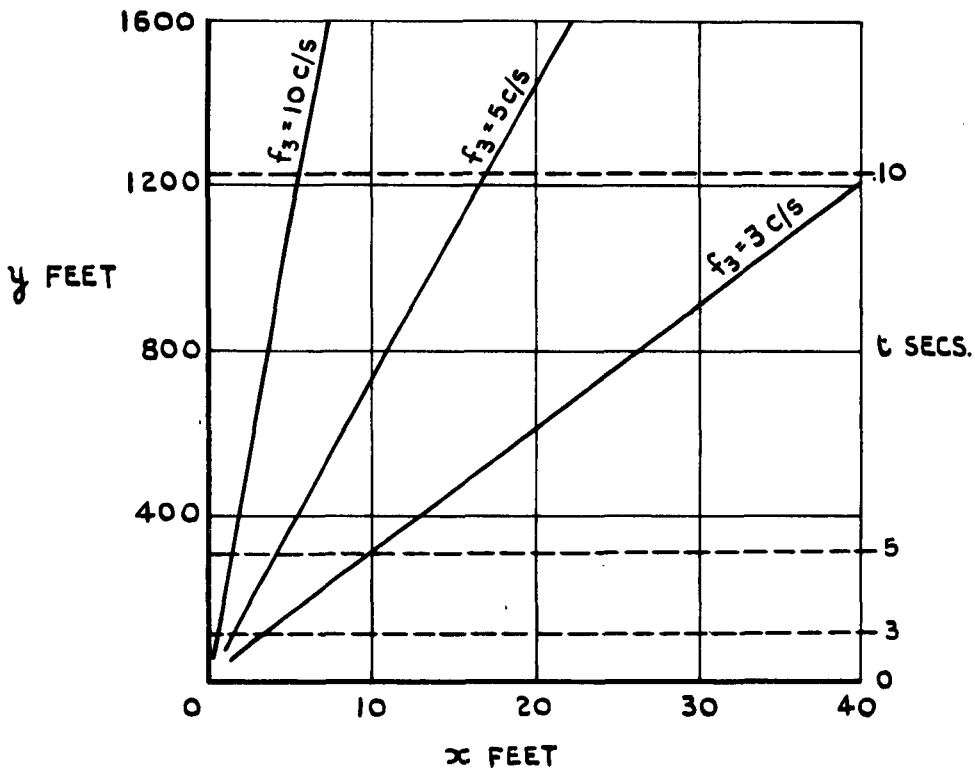

f_3 = SERVO BANDWIDTH

FIG.16. MISSILE TRAJECTORIES RESULTING FROM A CONSTANT ROCKET MOTOR DEFLECTION BIAS OF 1°, FOR THE CONTROL SYSTEM OF FIG.1. (WITHOUT INTEGRAL OF ERROR).

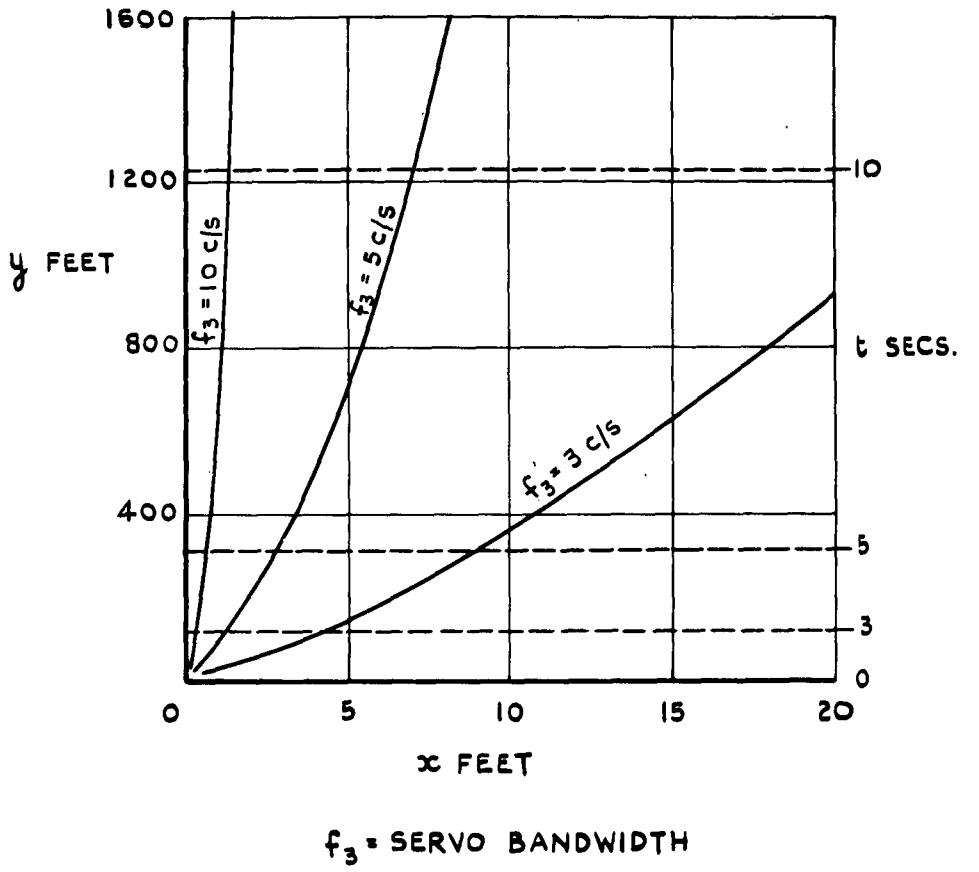

FIG.17. MISSILE TRAJECTORIES RESULTING FROM A CONSTANT ROCKET MOTOR DEFLECTION BIAS OF 1°, FOR THE CONTROL SYSTEM OF FIG.2. (WITH INTEGRAL OF ERROR).

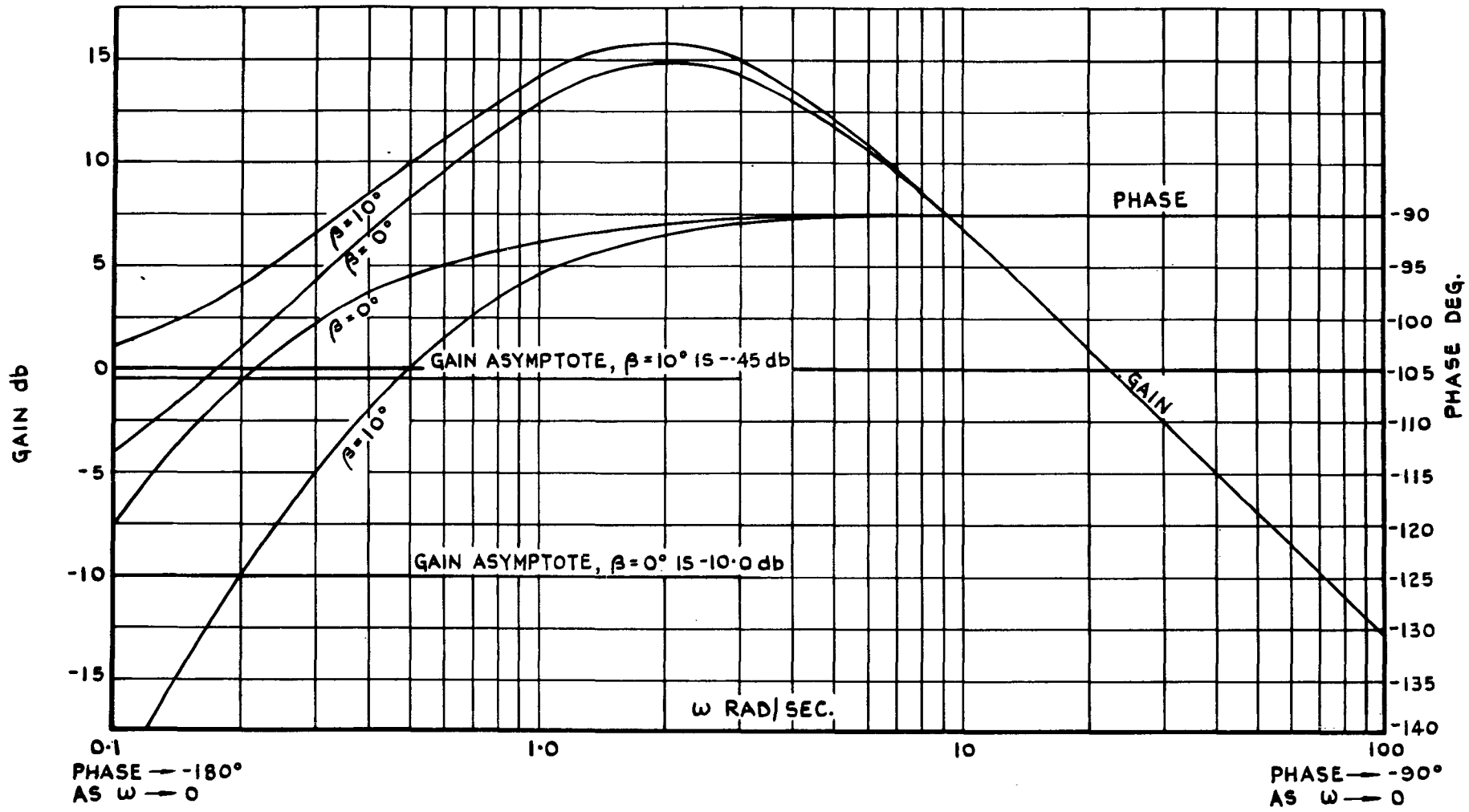

FIG.18. AERODYNAMIC FREQUENCY RESPONSE $(-K_4 G_4) = \frac{+\cdot 317\,(1+17\cdot 45\,p)}{(\cdot 494p-1)(\cdot 489p+1)}$ AT $\beta = 0°$

AND $= \frac{+\cdot 950\,(1+6\cdot 84p)}{(\cdot 550p-1)(\cdot 518p+1)}$ AT $\beta = 10°$.

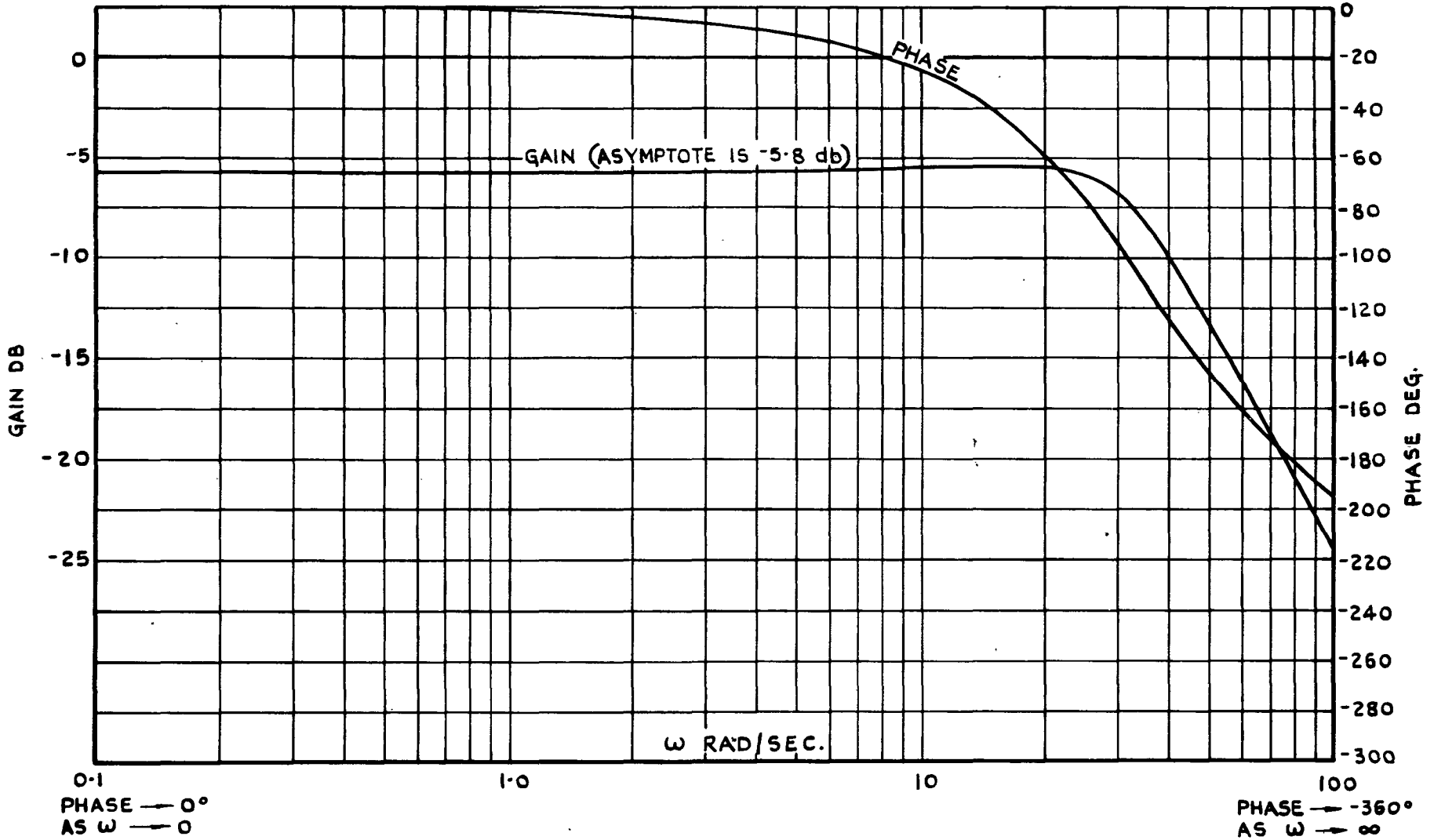

FIG. 19. COMBINED RESPONSE OF SERVO AND RATE GYROSCOPE ($K_2 G_2 K_3 G_3$)
(SERVO BANDWIDTH OF 5c/s., $K_2 = 0{\cdot}507$ AND $K_3 = 1$.)

T.N. G.W. 397.
FIG. 19.

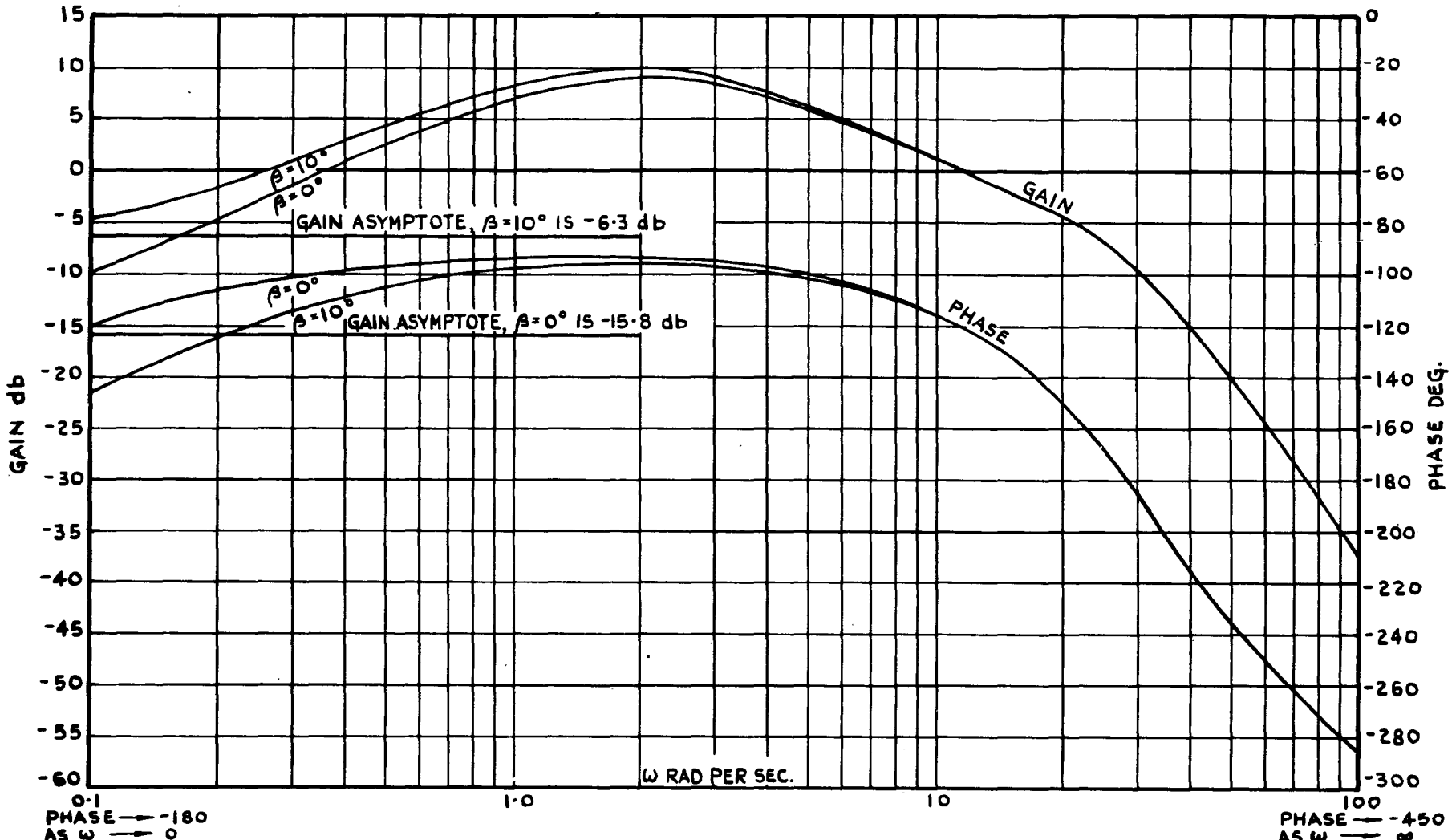

FIG.20. RATE FEEDBACK LOOP FREQUENCY RESPONSE ($K_2 G_2 K_3 G_3 K_4 G_4$) IN THE PRESENCE OF AERODYNAMICS. (SERVO BANDWIDTH OF 5 c/s. $K_2 = 0{\cdot}507$, $K_3 = 1$.)

GW/P/6945

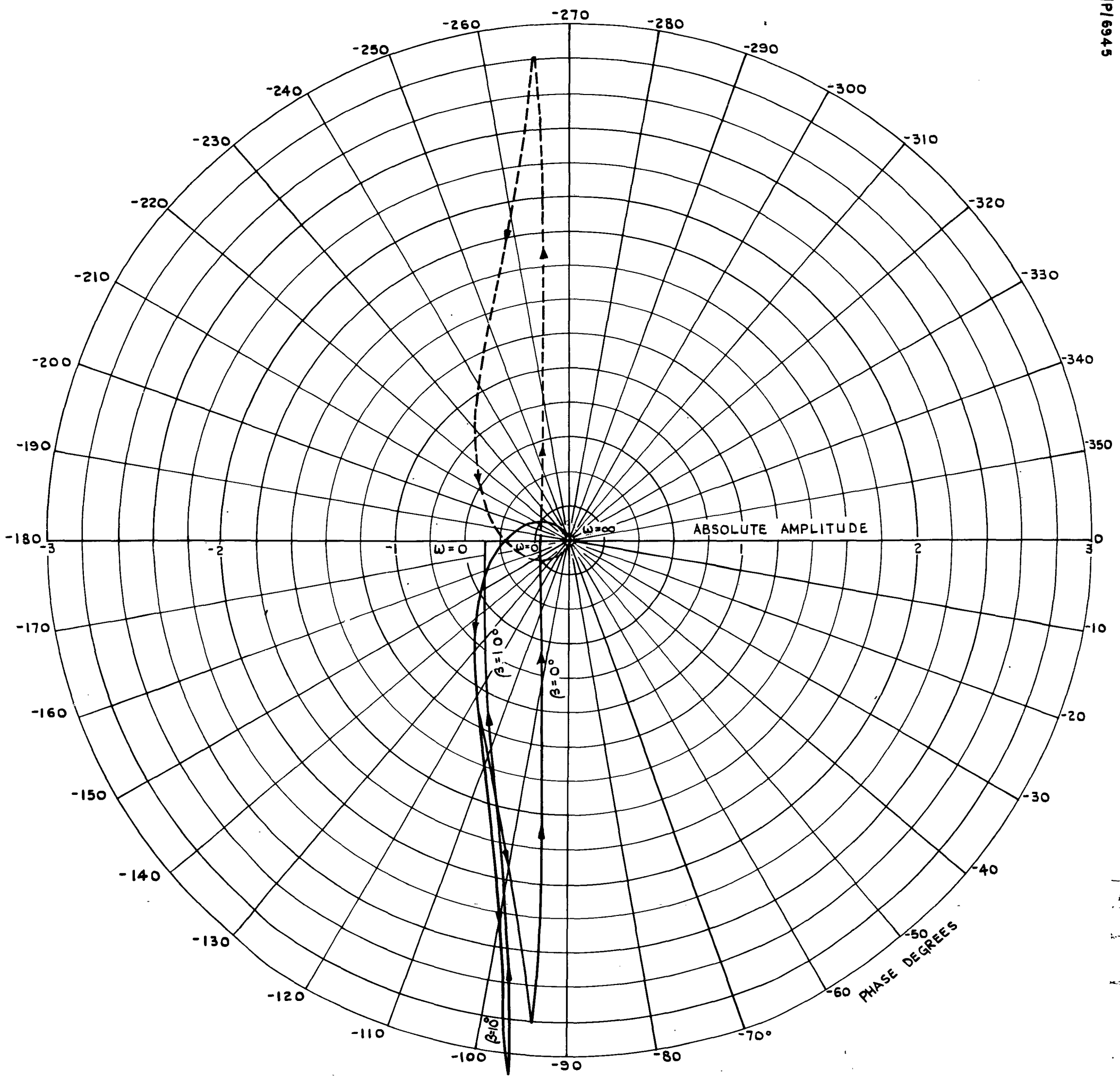

FIG. 21. NYQUIST DIAGRAM OF THE RATE FEEDBACK LOOP FOR THE CONTROL SYSTEM OF FIG. 2 IN THE PRESENCE OF AERODYNAMICS.

$(KG)_{\text{INNER LOOP}} = K_2 G_2 K_3 G_3 K_4 G_4$.

(CLOSURE FOR NEGATIVE FREQUENCIES AT $\beta = 0^\circ$ IS SHOWN BY BROKEN LINE.)

T.N. GW. 397.
FIG. 21.

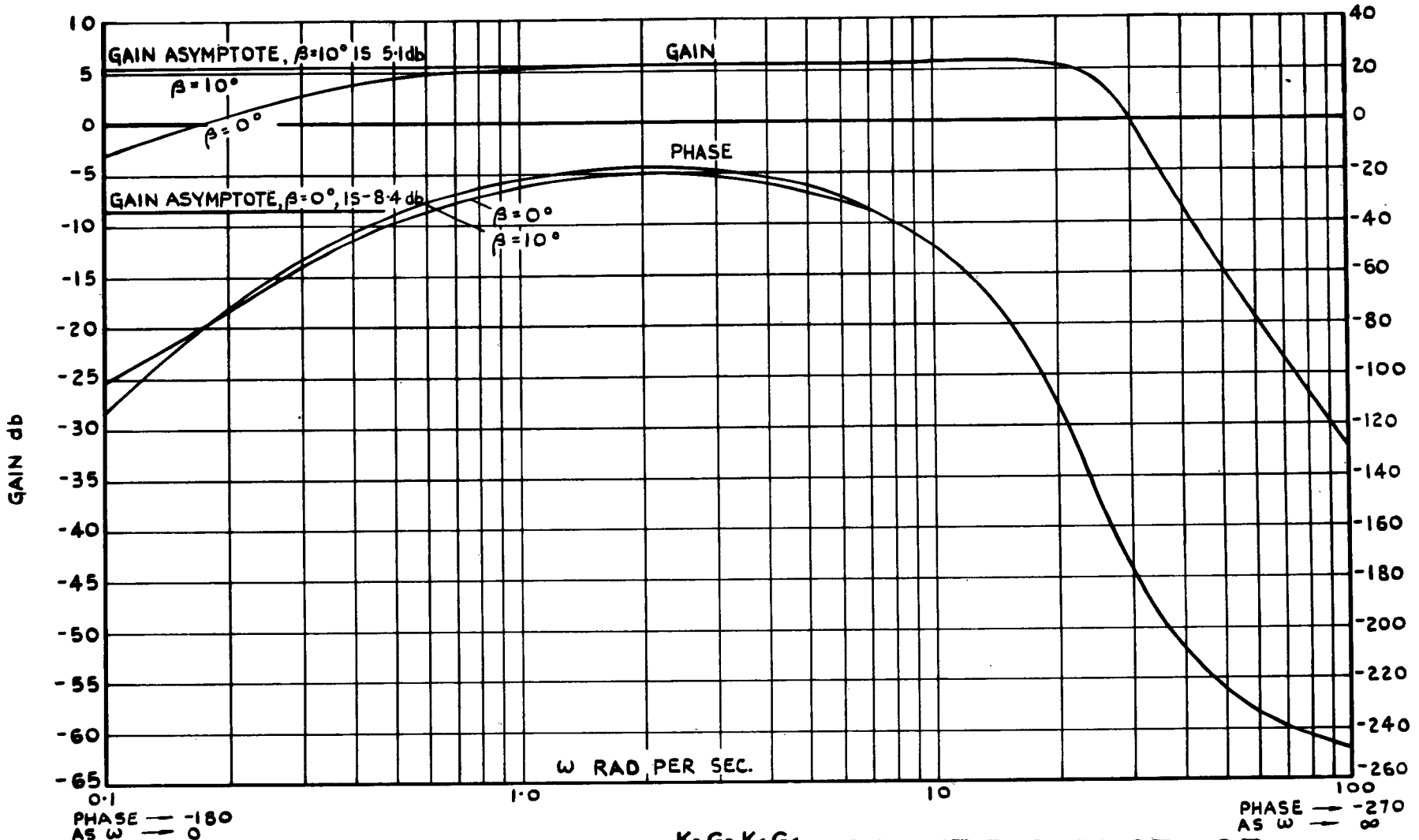

FIG.22. FREQUENCY RESPONSE OF $\frac{K_3 G_3 K_4 G_4}{1+K_2 G_2 K_3 G_3 K_4 G_4}$ IN THE PRESENCE OF AERODYNAMICS. (SERVO BANDWIDTH OF 5 c/s).

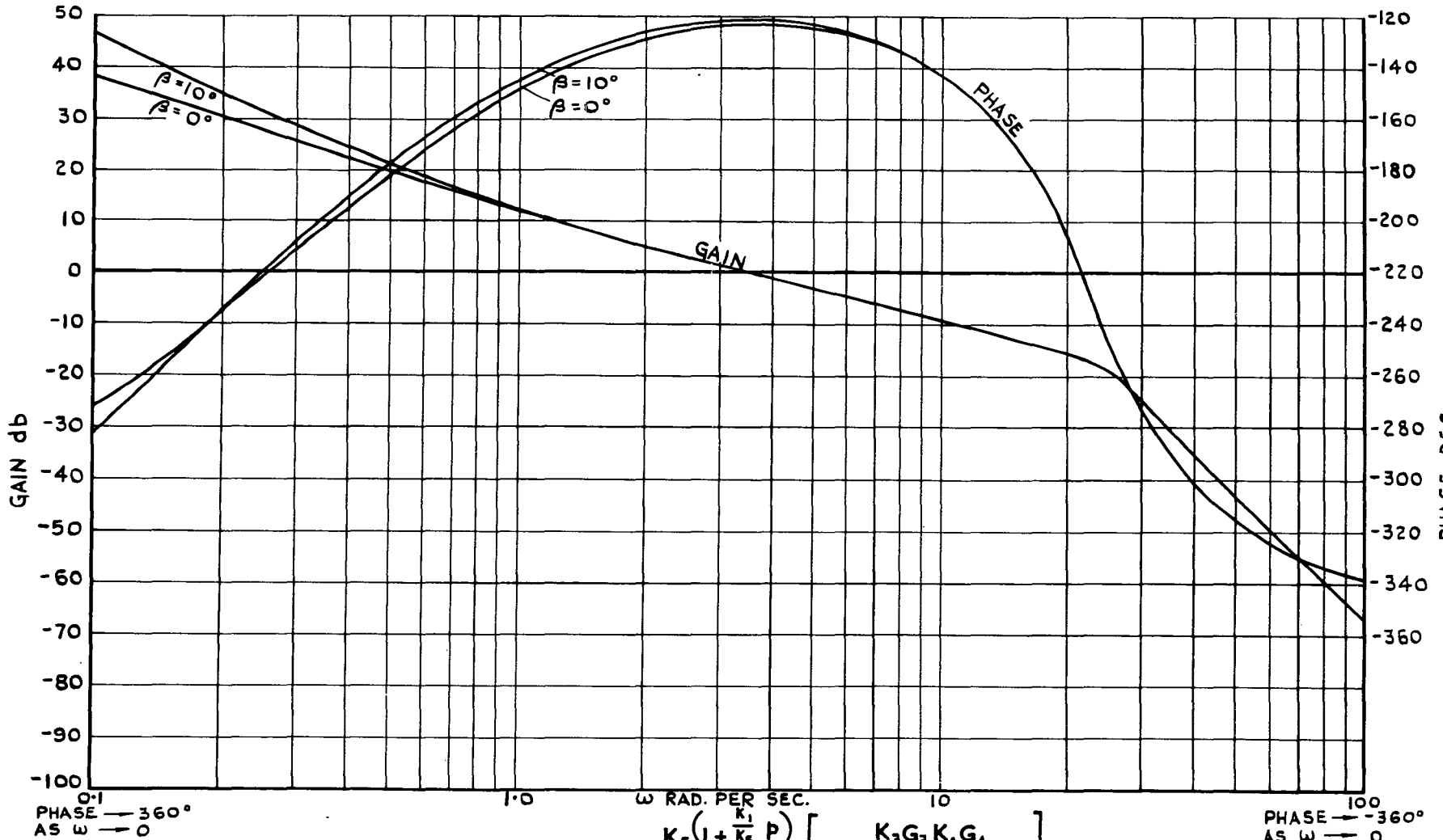

FIG.23. FREQUENCY RESPONSE OF $\frac{K_5\left(1+\frac{K_1}{K_5}P\right)}{P^2}\left[\frac{K_3G_3K_4G_4}{1+K_2G_2K_3G_3K_4G_4}\right]$ FOR THE OUTER LOOP OF THE CONTROL SYSTEM IN FIG.2 IN THE PRESENCE OF AERODYNAMICS. (SERVO BANDWIDTH OF 5 c/s).

TN. GW. 397.

FIG. 23.

FIG.24.

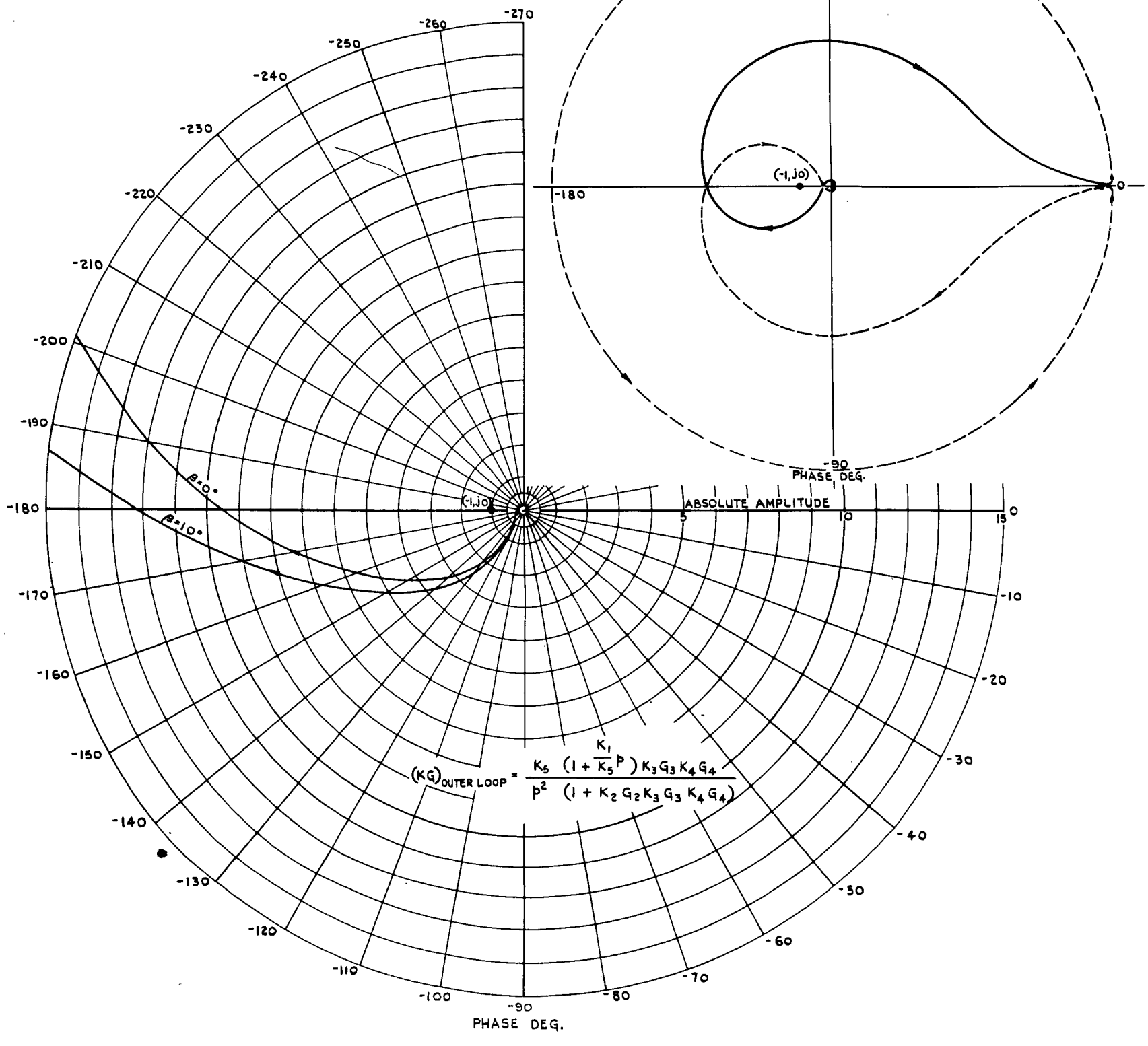

FIG.24. NYQUIST DIAGRAM OF THE OUTER LOOP FOR THE CONTROL SYSTEM OF FIG.2 IN THE PRESENCE OF AERODYNAMICS.

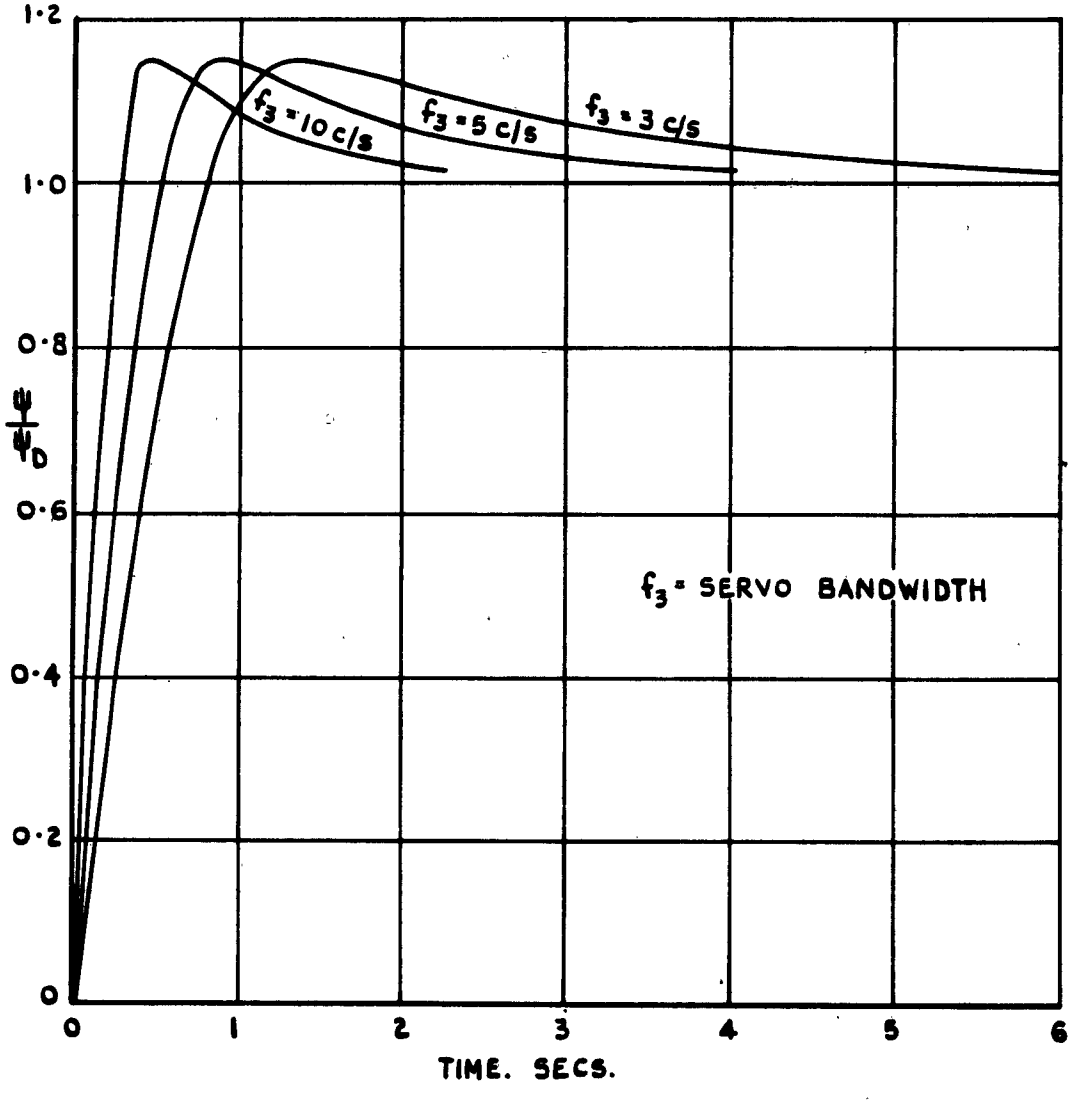

FIG. 25. MISSILE RESPONSE TO A STEP FUNCTION OF DEMANDED HEADING ANGLE ψ_D FOR THE CONTROL SYSTEM OF FIG. 2, NEGLECTING AERODYNAMICS.

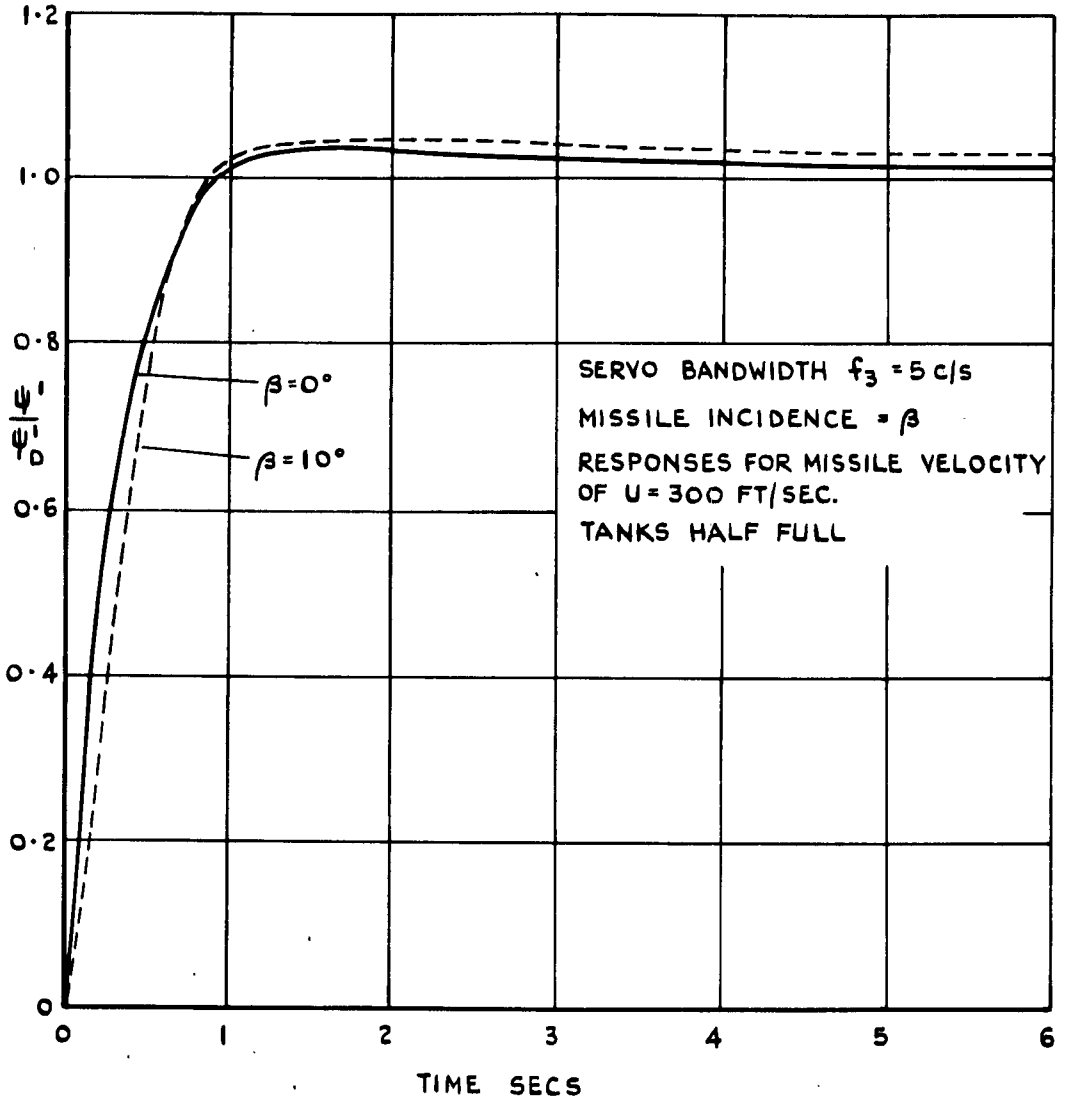

FIG. 26. MISSILE RESPONSE TO A STEP CHANGE OF DEMANDED HEADING ANGLE ψ'_D FOR THE CONTROL SYSTEM OF FIG. 2. IN PRESENCE OF AERODYNAMICS.

DETACHABLE ABSTRACT CARDS

These abstract cards are inserted in RAE Reports and Technical Notes for the convenience of Librarians and others who need to maintain an Information Index.

Detached cards are subject to the same Security Regulations as the parent document, and a record of their location should be made on the inside of the back cover of the parent document.

SECRET

Royal Aircraft Estab. Technical Note No. GW 397
1956.1
MacLaren, A. P. and Shannon, J. H. W.

623.451-519:
629.13.014.59:
533.691.155.8:
533.665

PRELIMINARY DESIGN AND ANALYSIS OF HEADING CONTROL SYSTEMS FOR A JET CONTROLLED TEST VEHICLE (RTV1 J)

As part of the supporting experimental programme for ballistic missile development, it is intended to control the heading of unboosted, vertically-launched, wingless RTV1 missiles by means of rocket motor deflection. A separate system of air jets will be used for roll stabilisation.

This note describes in some detail the preliminary design and analysis of the proposed pitch and yaw control system. Frequency response techniques are used in the basic design of the system. From this analysis, in which aerodynamic forces are neglected, suitable values of loop gain for a range of rocket motor servo bandwidths are determined. Two possible systems, with

SECRET P.T.O.

SECRET

Royal Aircraft Estab. Technical Note No. GW 397
1956.1
MacLaren, A. P. and Shannon, J. H. W.

623.451-519:
629.13.014.59:
533.691.155.8:
533.665

PRELIMINARY DESIGN AND ANALYSIS OF HEADING CONTROL SYSTEMS FOR A JET CONTROLLED TEST VEHICLE (RTV1 J)

As part of the supporting experimental programme for ballistic missile development, it is intended to control the heading of unboosted, vertically-launched, wingless RTV1 missiles by means of rocket motor deflection. A separate system of air jets will be used for roll stabilisation.

This note describes in some detail the preliminary design and analysis of the proposed pitch and yaw control system. Frequency response techniques are used in the basic design of the system. From this analysis, in which aerodynamic forces are neglected, suitable values of loop gain for a range of rocket motor servo bandwidths are determined. Two possible systems, with

SECRET P.T.O.

SECRET

Royal Aircraft Estab. Technical Note No. GW 397
1956.1
MacLaren, A. P. and Shannon, J. H. W.

623.451-519:
629.13.014.59:
533.691.155.8:
533.665

PRELIMINARY DESIGN AND ANALYSIS OF HEADING CONTROL SYSTEMS FOR A JET CONTROLLED TEST VEHICLE (RTV1 J)

As part of the supporting experimental programme for ballistic missile development, it is intended to control the heading of unboosted, vertically-launched, wingless RTV1 missiles by means of rocket motor deflection. A separate system of air jets will be used for roll stabilisation.

This note describes in some detail the preliminary design and analysis of the proposed pitch and yaw control system. Frequency response techniques are used in the basic design of the system. From this analysis, in which aerodynamic forces are neglected, suitable values of loop gain for a range of rocket motor servo bandwidths are determined. Two possible systems, with

SECRET P.T.O.

SECRET

Royal Aircraft Estab. Technical Note No. GW 397
1956.1
MacLaren, A. P. and Shannon, J. H. W.

623.451-519:
629.13.014.59:
533.691.155.8:
533.665

PRELIMINARY DESIGN AND ANALYSIS OF HEADING CONTROL SYSTEMS FOR A JET CONTROLLED TEST VEHICLE (RTV1 J)

As part of the supporting experimental programme for ballistic missile development, it is intended to control the heading of unboosted, vertically-launched, wingless RTV1 missiles by means of rocket motor deflection. A separate system of air jets will be used for roll stabilisation.

This note describes in some detail the preliminary design and analysis of the proposed pitch and yaw control system. Frequency response techniques are used in the basic design of the system. From this analysis, in which aerodynamic forces are neglected, suitable values of loop gain for a range of rocket motor servo bandwidths are determined. Two possible systems, with

SECRET P.T.O.

and without integral of error control, are considered and their relative merits are illustrated by comparing the deviations from a vertical trajectory caused by an initial heading error and a control system bias. These simplified trajectory calculations indicate that the control system including integral of error is to be preferred. In the final section, the effects of aerodynamic forces, under particular conditions of flight, on the stability of the proposed system are examined.

It is concluded that a stable heading control system for aerodynamically unstable RTV1 test vehicles can be developed along the lines proposed in this note, without demanding excessively high component performances. Further work will include studies of the effects of body flexure on the stability of the system and simulator tests in which some of the actual components will be incorporated in the control loop.

SECRET

and without integral of error control, are considered and their relative merits are illustrated by comparing the deviations from a vertical trajectory caused by an initial heading error and a control system bias. These simplified trajectory calculations indicate that the control system including integral of error is to be preferred. In the final section, the effects of aerodynamic forces, under particular conditions of flight, on the stability of the proposed system are examined.

It is concluded that a stable heading control system for aerodynamically unstable RTV1 test vehicles can be developed along the lines proposed in this note, without demanding excessively high component performances. Further work will include studies of the effects of body flexure on the stability of the system and simulator tests in which some of the actual components will be incorporated in the control loop.

SECRET

SECRET

and without integral of error control, are considered and their relative merits are illustrated by comparing the deviations from a vertical trajectory caused by an initial heading error and a control system bias. These simplified trajectory calculations indicate that the control system including integral of error is to be preferred. In the final section, the effects of aerodynamic forces, under particular conditions of flight, on the stability of the proposed system are examined.

It is concluded that a stable heading control system for aerodynamically unstable RTV1 test vehicles can be developed along the lines proposed in this note, without demanding excessively high component performances. Further work will include studies of the effects of body flexure on the stability of the system and simulator tests in which some of the actual components will be incorporated in the control loop.

SECRET

[dstl]

Defense Technical Information Center (DTIC)
8725 John J. Kingman Road, Suit 0944
Fort Belvoir, VA 22060-6218
U.S.A.

AD#: AD0093432

Date of Search: 22 Oct 2009

Record Summary: AVIA 6/19793
Title: Preliminary Design and Analysis of Heading Control Systems for a Jet Controlled Test Vehicle (RTV1 J)
Availability Open Document, Open Description, Normal Closure before FOI Act: 30 years
Former reference (Department): Technical Note, GW-397
Held by: The National Archives, Kew

This document is now available at the National Archives, Kew, Surrey, United Kingdom.

DTIC has checked the National Archives Catalogue website (http://www.nationalarchives.gov.uk) and found the document is available and releasable to the public.

Access to UK public records is governed by statute, namely the Public Records Act, 1958, and the Public Records Act, 1967.
The document has been released under the 30 year rule.
(The vast majority of records selected for permanent preservation are made available to the public when they are 30 years old. This is commonly referred to as the 30 year rule and was established by the Public Records Act of 1967).

This document may be treated as UNLIMITED.